



Finite Element Analysis of
Custom Tri-Flange Acetabular Cups

By

Ella Fairweather

Thesis

Submitted to Flinders University

for the degree of

Master of Engineering (Biomedical) – 18 Units

College of Science and Engineering

June 2022

Table of Contents

Table of Contents	ii
Executive Summary	v
Declaration.....	vi
Acknowledgments.....	vii
List of Figures.....	viii
List of Tables.....	x
1 Introduction	1
1.1 Background Information	1
1.1.1 Custom Tri-Flange Acetabular Cups.....	1
1.1.2 Production Process	2
1.2 Failure Mechanisms	3
1.3 Research Aims.....	4
1.4 Project Scope and Methodology	4
2 Literature Review.....	6
2.1 Custom Triflange Acetabular Component Fixation Methods	6
2.1.1 Component Loosening	6
2.1.2 Screw Orientation.....	7
2.2 The Finite Element Study.....	9
2.2.1 Screw Geometry.....	10
2.2.2 Material Properties	10
2.2.3 Modelling Implant – Bone Interactions	11
2.2.4 Forces in the Hip Joint and Boundary Conditions	11
3 Project Methodology	13
3.1 Project Plan	13
3.2 The Finite Element Model.....	13

3.2.1	Pelvis and Custom Triflange Acetabular Cup.....	13
3.2.2	Proposed Screw Orientation.....	14
3.2.3	Components.....	14
3.3	Mesh Generation	15
3.3.1	Material Properties	16
3.3.2	Component Interactions	17
3.3.3	Applied Load.....	17
3.3.4	Boundary Conditions.....	17
3.4	Simulations.....	18
3.4.1	Achieving the Aim	18
3.4.2	Graft Material Properties Verification Study	18
3.5	Data Analysis	19
3.6	Mesh Refinement Study	19
4	Normal Force Distribution with Nominal Load	21
4.1	Results	21
4.1.1	1 st Trial Group: All Screws Active.....	21
4.1.2	2 nd Trial Group: Suppress 1 Screw at a Time.....	22
4.1.3	3 rd Trial Group: Suppress 2 Screws at a Time	22
4.2	Discussion	23
5	Normal Force Distribution during a Complete Gait Cycle	27
5.1	Results	28
5.1.1	1 st Trial Group: All Screws Active.....	28
5.1.2	2 nd Trial Group: Suppress 1 Screw at a Time.....	29
5.1.3	3 rd Trial Group: Suppress 2 Screws at a Time	29
5.2	Discussion	30
6	Graft Material Properties.....	34
7	Discussion, Limitations and Future Work.....	36

7.1	Discussion	36
7.2	Limitations and Assumptions.....	37
7.3	Future Work	39
8	Conclusion.....	41
9	References	42
10	Appendices	47
	Appendix I: Illustration of the human pelvic girdle	47
	Appendix II: Screw Plan	48
	Appendix III: Mesh Generation	49
	Appendix IV: Mesh Properties.....	50
	Appendix V: MATLAB Code.....	53
	Appendix VI: Gantt Chart.....	57

Executive Summary

Custom tri-flange acetabular components (CTAC) are frequently utilised to treat a revision total hip arthroplasty (THA) where significant acetabular bone defects are present. Approximately 10% to 15% of THA cases will undergo a revision, with the most common failure mechanism being aseptic loosening due to poor bone quality of the pelvis (Sculco et al., 2022). Poor bone quality of the host bone can result in inadequate primary stability of an implant as it is difficult for the fixation methods utilised to gain fixation. Fixation methods of a CTAC to the pelvis generally consists of a number of screws supported by three flanges. From the literature, it can be suggested that there is over-compensation of the number screws to obtain primary stability of the implant. Over-compensation can lead to further deterioration of the pelvis, especially if multiple revisions are required.

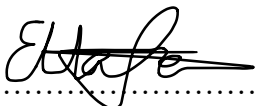
The challenge that surgeons face is gaining fixation of multiple screws into the host bone intraoperatively to gain primary stability of the implant. Finite element analysis (FEA) was utilised in this study to present evidence of the force transmission into the screws under two mechanical loading conditions. A total of seven screws were modelled, where screw number 1 was fixated into the pubis, screws number 2 and 3 in the ischium and screws number 4-7 in the ilium. These conditions simulated a nominal load applied to the femoral head and a peak contact force on the femoral head during a complete gait cycle. The aim of the thesis was to identify which screws are important in achieving primary fixation under the applied load conditions. The results from this study provided evidence to suggest that suppressing screws number 3 and 4 in the ischium and ilium respectively had the least effect on the transmission to the applied load in remaining screws. Omitting screws number 3 and 4 from the screw plan will aid in the restoration of bone quality without impacting the load transmitted into the remaining screws. Finally, this study proved that the screws with greater force per millimetre of length of screw while all screws were active (screws 2 and 5 under the peak contact force during a complete gait cycle), when removed, had potentially detrimental effect on the remaining screws and overall load transfer.

Declaration

I declare that this thesis has been composed solely by myself and that it has not been submitted, in whole or in part, in any previous application for a degree or diploma in my name and to the best of my knowledge, contains no material previously published or written by another person. I certify that the research within will not be submitted for any future degree of diploma without the permission of Flinders University. There is an exception where states otherwise by reference or acknowledgment, the work present is entirely my own.

Ella Fairweather

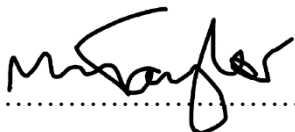
Master of Engineering (Biomedical) – Flinders University, Adelaide, South Australia

Signed:

Name: Ella Fairweather

Date:30/05/2022.....

I declare that I have read this thesis. In my opinion it is fully adequate, in scope and in quality as a thesis for the degree of Master of Engineering (Biomedical). Furthermore, I confirm that I have provided feedback on this thesis and the student has implemented it fully.

Signed:

Name: Professor Mark Taylor

Date:02/06/2022.....

Acknowledgments

I would like to thank and acknowledge the continued guidance and advice from my project supervisor Professor Mark Taylor, in association with assistance from Mr Dermot O'Rourke and Ms Daniela Mini – all at Flinders University. Their guidance has enabled me to complete this thesis within the timeframe, obtain and understand the results produced. The dedication towards enhancing biomedical research and study expressed by these individuals is outstanding and has given me the motivation to improve and develop as both a researcher and technical writer.

List of Figures

Figure 1.1: Custom Tri-Flange Acetabular Cup (Zimmer Biomet, 2022)	1
Figure 1.2: Component Migration (Berend et al., 2018).....	2
Figure 1.3: Development Process of a CTAC (Gruber et al., 2020) - (a) initial pelvis model, (b) bone defects, (c) CTAC design, (d) Bone graft	3
Figure 1.4: Computed Tomography Scan provided by OSSIS	5
Figure 2.1: Considerable ischial pulloff and mechanical failure of CTAC (Wind et al., 2013)	6
Figure 2.2: Proposed screw orientation (Berend et al., 2018 – Left, Abdel et al., 2017 – Right).....	8
Figure 2.3: Hip joint contact forces during walking (Damm et al., 2015).....	12
Figure 3.1: Project Plan.....	13
Figure 3.2: Computed Tomography scan of the patient (left) and constructed pelvis (pink) and implant (blue) from CT scan (right)	14
Figure 3.3: Components and screw orientation of the Finite Element Model	15
Figure 3.4: Load applied perpendicular to the surface of the femoral head (left) and boundary conditions (right).....	18
Figure 3.5: Mesh refinement under nominal load	19
Figure 4.1: Force distribution when all screws active for first trial group.....	21
Figure 4.2: Force distribution in the screws for second trial group	22
Figure 4.3: Force distribution in the screws for third trial group.....	23
Figure 4.5: Screw number 1 suppressed (left) & screw number 7 suppressed (right)	24
Figure 4.4: Force per millimetre of length when all screws were active	24
Figure 4.6: Screws number 6 and 7 suppressed (left) and screws number 4 and 7 suppressed (right).....	25
Figure 4.7: Screws number 1 and 7 suppressed (left) and screws number 3 and 5 suppressed (right).....	26
Figure 5.1: Force distribution when all screws are active under peak contact force	28
Figure 5.2: Force distribution suppressing one screw at a time under a peak contact force.....	29
Figure 5.3: Force distribution suppressing two screws at a time under peak contact force.....	30
Figure 5.4: Force per mm within the screws.....	31

Figure 5.5: Screw no. 2 suppressed (left) & screw no. 5 suppressed (right).....	31
Figure 5.6: Screws number 4 suppressed (left) & screws number 3 & 4 suppressed (right).....	32
Figure 5.7: Screws number 2 & 3 suppressed (left) & screws number 4 & 5 suppressed (right).....	33
Figure 6.1: The effect on force distribution in screws when the graft material properties are changed ...	34
Figure 6.2: Relationship between graft Young's Modulus and total force within screws	35
Figure 10.1: Pelvic Girdle (Samanthi, 2013)	47
Figure 10.2: Screw Plan with Lengths	48
Figure 10.3: Mesh generation on all components	49
Figure 10.4: Mesh properties for coarseness set to -5.....	50
Figure 10.5: Mesh properties for coarseness set to -10.....	51
Figure 10.6: Mesh properties for coarseness set to +10.....	52
Figure 10.7: Gantt Chart.....	57

List of Tables

Table 3.1: Material Properties	16
Table 3.2: X, Y & Z components of applied force	17

1 Introduction

1.1 Background Information

Approximately 10% to 15% of total hip arthroplasty (THA) patients will undergo a revision at 20 years post-surgery, with the most common cause being aseptic loosening of the acetabular components (Sculco et al, 2022). Consequently, failure of a THA can lead to significant acetabular bone loss. The reconstruction of failed acetabular components and management of acetabular bone loss is one of the most complex problems in orthopaedic surgery (Issak et al., 2009). Custom triflange acetabular component's (CTACs) have increased in popularity for the treatment of a revision THA where significant acetabular bone loss and defects is evident.

1.1.1 Custom Tri-Flange Acetabular Cups

The triflange acetabular component is a patient-specific implant that is designed to treat a Total Hip Arthroplasty where significant acetabular bone loss exists. The three-dimensional printed implants are typically made from titanium with a hydroxyapatite coating to facilitate osseointegration into the host bone. The design of a CTAC consists of three flanges that sit on the ilium, ischium and pubis (Figure 1.1). These rigid flanges protrude from the cup and provide areas of contact for fixation onto the host bone (on the ilium, ischium and pubis – see appendix I for illustration of the human pelvis girdle) (Goodman, 2016). The flanges also facilitate screw fixation to provide stability of the implant (Goodman, 2016). CTAC are cementless implants and rely on osseointegration of both implant and screws into the pelvis to provide long-term stability postoperatively. To provide primary stability, the implant is fixed to the pelvis using a number of screws where the orientation and number of screws are determined in partnership between the surgeon and manufacture.

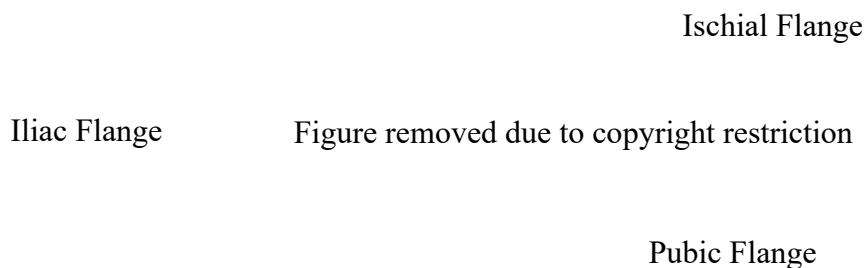


Figure 1.1: Custom Tri-Flange Acetabular Cup (Zimmer Biomet, 2022)

High failure rates of a total hip arthroplasty exist due to inadequate fixation of the acetabular components to the host bone (Matar et al., 2020). An example of component migration post-surgery can be observed in Figure 1.2 where the left acetabular components have significantly migrated towards the abdomen.

Figure removed due to copyright restriction

Figure 1.2: Component Migration (Berend et al., 2018)

Acetabular loosening and component migration can lead to life threatening injuries on the individual, specifically the protrusion of the implant into the pelvis cavity (Kotela et al., 2020) which increases the risk of damage to the anatomic structures in this region. Significant damage to these structures can have a detrimental effect to vital organs located in the body and the loss of hip centre of rotation (Eemeren et al., 2020). Studies have demonstrated that cases where multiple THA revisions have occurred or in women with a smaller pelvis, are at higher risk to requiring a CTAC (Christie, 2016).

Custom tri-flange components are indispensable as they provide surgeons with the ability to adequately fix the acetabular components required for a total hip arthroplasty to the pelvis, particularly where significant bone loss exists. Often used in conjunction with a bone graft, which acts as a filler between the implant and host bone, the objective of a CTAC is to span the acetabular defect and obtain fixation to the host bone (Goodman, 2016). In addition, the patient will benefit from a CTAC as it will provide better restoration of the natural biomechanics within the pelvis.

1.1.2 Production Process

The production process of developing a CTAC commences with a computed tomography (CT) scan of the patient where a computer-generated model of the pelvis is generated (Figure 1.3 – a) (Wind et al., 2013). The bone defect is assessed (Figure 1.3 – b) and the custom implant is designed in partnership between the surgeon and manufacture from the pelvis model (Figure 1.3– c) (Martino et al., 2019). These models are substantially more accurate than other methods of determining the bone defects within the perioperative plan (Goodman & Engh, 2016). The surgeon will select the location, orientation and number of screws to adequately fix the implant to the host bone. Furthermore, when the design is agreed upon, the computer aided design (CAD) files are sent to be 3D printed to create the implant. A significant difference of the production process between a CTAC and other acetabular reconstruction techniques is that pelvic discontinuities and bone defects are recognised prior to surgery which facilitates the design and production of the implant. Having knowledge of the bone defects prior to surgery can aid in a more successful procedure.

Figure removed due to copyright restriction

(a) (b) (c) (d)

Figure 1.3: Development Process of a CTAC (Gruber et al., 2020) - (a) initial pelvis model, (b) bone defects, (c) CTAC design, (d) Bone graft

In addition to the custom implant, where there are catastrophic bone defects in the pelvis, a bone graft may be modelled (Figure 1.3 – d, indicated by the red shaded area). From the model, the bone deficiencies can be identified and supplemented with bone graft which will aid in the restoration and increase the quality of the bone (Berend et al., 2018). The introduction of a bone graft can provide rigid fixation of the implant to the bone (Berasi et al., 2014) and further decrease the risk of component migration.

1.2 Failure Mechanisms

As reported in literature, the overall complication rate of CTACs is 26% (Eemeren et al., 2020). One of the major challenges evident with the use of CTACs is determining the orientation and number of screws that are utilised to provide primary fixation and decrease the risk of aseptic loosening. Careful consideration must be given into the screw location and type of screw within the perioperative plan. There are many factors that need to be considered when selecting the location of a screw including bone quality, bone depth, screw length, other anatomic structures in the vicinity, physiological loading on the screw, desired screw compression and the ability to gain adequate exposure for successful drilling (Zimmer Biomet, 2011). Incorrect placement and fixation of these screws can lead to component migration and hence a failed CTAC. Despite extensive perioperative planning, Baauw et al. highlighted the difficulty of positioning a custom-made implant and screws accurately intraoperatively in patients with large acetabular defects (Baauw et al., 2015).

In any bone-screw interaction, there are three main mechanisms of failure: screw loosening, stripping and fracture. When CTACs are utilised, there is generally significant bone defects in the vicinity of the bone-screw interaction. Therefore, it is particularly difficult to gain fixation of a CTAC. There is a gap in literature that determines which of the screws are withstanding the most load and therefore, which screws are necessary for fixation. Additionally, there is evidence to suggest that within the perioperative plan, there is over-compensation of the number of screws to ensure this fixation and to further decrease the risk of aseptic loosening. Since CTAC are utilised specifically when there is significant bone loss and defects in the pelvis, overcompensation of the number of screws can lead to further deterioration of the host bone. This is particularly evident when a failure mechanism of the screw occurs.

1.3 Research Aims

The overall aim of this project was to develop a deeper understanding of the force distribution found within the screws that are utilised to fixate a CTAC to the pelvis and subsequently observe the effect of this force distribution when screws do not gain fixation. This main aim can be split into three underlying aims which the project will endeavour to achieve.

- (1) **Model** the pelvis and the different components that are required for a total hip arthroplasty. This consists of appropriately generating the mesh of components, assigning material properties and setting up the Finite Element (FE) model.
- (2) **Quantify** the load present in each of the screws under an applied load.
- (3) **Identify** which of the screws are withstanding the most load. Additionally, identify which screws, when suppressed (this simulates when the screw does not become fixed to the bone) in the FE model have the least effect on the transmission of load into the remaining screws.

Achieving these aims will provide both the surgeons and manufactures an understanding of which screws need to gain fixation into the host bone to ensure primary stability and reduce the risk of CTAC failure. Ensuring component fixation will lead to a greater chance of restoration of hip biomechanics and hence, a successful revision.

1.4 Project Scope and Methodology

The scope of the project can be summarised by a finite element (FE) analysis on the model which consists of the components found in a total hip arthroplasty. These components include the femoral head, a polyethylene liner which sits between the femoral head and the CTAC, screws, a bone graft and the pelvis. The geometry and anatomy of the CTAC and pelvis are specific to one individual and supplied by OSSIS, a New Zealand company specialising in custom implants. OSSIS provided the case with a CTAC to treat a THA. The patient had undergone a THA and significant acetabular component migration occurred towards the abdomen which can be observed in Figure 1.4. Additionally, it can be recognised that there is significant bone deterioration in the left pelvis which was hindered further by the acetabular component migration. There are no ethical concerns with utilising the scans from this case. Simulations of the FE model were run to determine the distribution of force within the screws that are utilised to fixate the CTAC to the pelvis and the effect of suppressing screws were investigated in order to achieve the project aims. Furthermore, for a sanity check a verification study was conducted focussing on the influence of the graft material properties and mesh refinement.



Figure 1.4: Computed Tomography Scan provided by OSSIS

2 Literature Review

2.1 Custom Triflange Acetabular Component Fixation Methods

For any surgery that involves an implant, fixation of the components to the host bone is key for success. Fixation will provide adequate stability post-surgery to allow the implant to osseointegrate into the bone. If primary stability is compromised, the implant micromotion can inhibit the osseointegration into the host bone (Finnila et al., 2015). The fixation of custom tri-flange acetabular components (CTACs) generally involves the use of bone screws and supported bone graft. Since CTAC are utilised when there is significant bone loss and deterioration in the pelvis, gaining implant fixation can be difficult.

2.1.1 Component Loosening

The most common complications associated with utilising a CTAC are component loosening, component migration, alteration of gait biomechanics, changes in the centre of rotation within the hip and dislocation (Wind et al., 2013). Wind et al., presented an investigation into the short-term results of CTACs for massive acetabular bone loss. Out of the 19 patients, three (16%) experienced major complications postoperative, where the most significant complications were mechanical failure which can result in loosening of the implant. In four (21%) patients, considerable migration of the implant involving pulloff from the ischium was evident (Figure 2.1). Additionally, in three (16%) patients, a fractured screw was present but no presence of component migration (Wind et al., 2013). This inadequate component fixation rate is supported by Holt and Dennis where component failure occurred in three (12%) patients predominantly due to loss of ischial fixation (Holt and Dennis, 2004). Furthermore, Taunton et al. found CTAC migration in nine (16%) patients (Taunton et al., 2012).

Figure removed due to copyright restriction

Figure 2.1: Considerable ischial pulloff and mechanical failure of CTAC (Wind et al., 2013)

Treatment success and fixation can be significantly hindered by the amount and quality of remaining bone stock (Froschen et al., 2020). Patients that have compromised bone quality have shown a significant risk of increased migration of acetabular components (Finnila et al., 2015). The use of a CTAC has shown promising long-term results once osseointegrated, however when the bone stock is insufficient, there are still concerns about primary implant stability (Myncke et al., 2017). During primary stability, the stability of the implant relies on the interlocking mechanism and frictional bone-implant phenomena to withstand the mechanical loading on the implant (Steiner et al., 2014). Strong evidence exists in the literature that fixation screws show a reduced mechanical competence immediately after implantation (primary stability) in patients with low bone quality (Steiner et al., 2014). There has been no clinical study observing the effect of bone quality on a CTAC fixation, however there is evidence to suggest that surgeons are reluctant to implant the cups when the bone quality is poor due to risk of failure.

A method that has been utilised to increase bone quality and component fixation is the addition of a bone graft. Introducing a bone graft will aid to reconstruct the defects and restore anatomic positions (Waddell et al., 2017). A major advantage of bone grafts is that the bone can be reshaped to exactly match the bone defect (Nieminen et al., 2013) which is aided by modelling the graft in the perioperative plan. Additionally, the locomotion of the pelvis can be fully restored (Nieminen et al., 2013). Waddell et al. stated that after 10 years, 90% of the grafts had incorporated into the host bone (Waddell et al., 2017). Cortical bone grafts have the ability to offer immediate load-bearing resistance due to their resistance to compressive loading (Roberts & Rosenbaum, 2012). However, there are complications that are associated with the use of bone grafts. Nieminen et al reported an overall complication rate of 30% to 90% due to mechanical failure as resorption and fragmentation was observed to occur within 5-10 years, in addition to high rates of infection (Nieminen et al., 2013).

2.1.2 Screw Orientation

Extensive perioperative planning is required to ensure the CTAC will span and reinforce the pelvic deficiencies evident in patients (Sculco et al., 2022). The minimum number and location of the screws needed for fixation is not defined but knowing the quality of host bone will guide where to place the screws for fixation (Sculco et al., 2022). The bone along the rim of the acetabulum tends to be the highest bone quality in the region, whereas due to the narrow bicortical thickness in the iliac spine, this provides the lowest bone quality and hence questionable screw fixation (Barlow et al., 2016). However, the centre of the ilium provides the best bone quality and the largest surface area for contact (Christie, 2013). Adequate fixation in the ischial region is critical since this site is the most common for pulloff (Figure 2.1). The bone quality in the ischium is generally poor which leads to poor screw fixation (Taunton et al., 2012) Investigations into the failure mechanisms of CTAC by Martino et al. showed an aseptic loosening

incidence of 3.1%. The pattern of failure was loosening of ischial screws where disengagement of the ischial flange was reported (Martino et al., 2019).

Incorrect screw orientation can lead to damage of the superior gluteal nerve and the sciatic nerve which is a common result of ischial screw loosening (Barlow et al., 2016). When using a posterior approach for implantation, the ischial flange sits under the sciatic nerve (Christie, 2016) which can cause nerve irritation. Due to the risk of nerve irritation established by screw fracture and failure, Kosashvilli et al. suggested that fixation using screws into the ischium should be limited (Kosashvilli et al., 2009). A study performed by Berend et al. investigated the fixation of patient specific triflange acetabular implants in a total of 94 patients between May 2004 and March 2016. The fixation of the implant utilised an average of 12 screws, out of those 12 screws, it was presented that an average of 3 screws were classified as locking screws (Figure 2.2 – Left) (Berend et al., 2018).

A locking screw enhances fixation and stability of the implant to the host bone by having two corresponding threads; one in the screw hole of the implant and the other on the head of the screw. When tightened, the thread on the screw head engages with the thread on the plate and locks the screw to the plate (Surgery Reference, 2022).

Christie proposed a plan of five to six screws in the iliac flange due to the large bone surface area and enhanced bone quality, three to four screws in the ischial flange and no screws in the pubic flange (Christie, 2016). Abdel et al. supported Christie by suggesting that 9-13 screws are required for fixation and additional screws should only be introduced through the ischium and pubis to prevent the cup from failing in abduction (Figure 2.2 – Right) (Abdel et al., 2017).

Figures removed due to copyright restriction

Figure 2.2: Proposed screw orientation (Berend et al., 2018 – Left, Abdel et al., 2017 – Right)

To date, there are several studies that present the failure scenarios occurring with the use of CTAC but no detail on the mechanisms that result in such failures. To our knowledge, there is, no literature or investigations into the force distribution within the screws to determine which screws are withstanding the most load and hence, highlighting which screws and the orientation that are required to gain adequate fixation. By gaining adequate fixation between the screws and pelvis, it will increase the primary stability of the implant which would enhance the durability, function and complication rate of these implants (Gladnick et al, 2018). Therefore, would solely influence the incidence rate of CTAC which are utilised to treat severe acetabular defects.

2.2 The Finite Element Study

Finite element analysis (FEA) has become a highly sort out tool to analyse stress, strain and the mechanical environment within structures under a static or dynamic load (Weiding et al., 2012). It offers an alternative method to experimental testing (in vitro) as it can perform multiple reproducible tests without damaging the specimen. Additionally, in vitro testing can often be time-consuming, expensive and accurate results can be hard to produce without expensive equipment. To produce an accurate model to perform FEA, there are several considerations that need to be made. Ultimately there are five main steps in the methodology to create the finite element (FE) model; generating the geometry of components, assigning material properties, component interactions, applied force and boundary conditions (Steiner et al., 2014). Review of previous studies will provide an insight into the methodology for assigning these modelling parameters.

A limited number of finite element studies have been performed focussing on the mechanical environment within a custom implant fixed to the pelvis. The distribution of stress in polyethylene acetabular lines was demonstrated in Kaku et al. (2020). This study produced evidence that increasing the area of contact of the liner positively affects the stress distribution within both liner and bone (Kaku et al, 2020). Maslov et al. (2021) presented a study comparing the stress distribution within the pelvis under different screw forces. It found that the highest stresses in the model occurred in the screws and the implant and when the screw forces increase, the local bone tissue has a greater risk of deterioration (Maslov et al., 2021). Another analysis into the strength and stability on custom prosthesis utilised in the pelvis was conducted by Dong et al. (2018). The methods utilised in this study involved a finite element model focussing on the pre-stress of the screws and the biomechanical performance of the reconstructed pelvis. Additionally, four of the fourteen screws were removed from the pelvic system and the results show that this did not affect the fixing stability (Dong et al., 2018). Although, this study was not regarding a custom tri-flange implant, the results have shown that the implant was fixated using too many screws as the magnitude and distribution of stresses were basically the same for the two trails. This indicates that four of the screws can be removed without comprising the stability of the implant (Dong et al, 2018). All these studies focussed on acetabular

reconstruction where there are significant defects within the hip. However, there have been no findings in the literature that utilises finite element methods to determine the force distribution and mechanical environment within a CTAC, particularly the effect on the force distribution when fixation fails.

2.2.1 Screw Geometry

A common approach to modelling screws in an FE model is utilising three-dimensional solid elements (Weiding et al., 2012) to reduce complexity of the geometry. Incorporating screw threads into the model would be a more realistic representation. However, studies have shown that the geometry of the screws can be approximated by cylindrical shapes with the consideration of the drill holes prior to meshing (Moazen et al., 2013). The approach of modelling the threads significantly increases the computationally expense since higher mesh densities are required to gain realistic mechanical behaviour. Generalisation of the screw geometry is supported by Chatzistergos et al. where the cylindrical models reproduced the same apparent stiffness of the threaded model geometry (Chatzistergos et al., 2010).

2.2.2 Material Properties

Throughout literature, there are varying methods and values for assigning material properties to bone. Several studies have determined the mechanical properties from the greyscale value on a CT scan (Razi et al., 2014). In a CT scan, the Hounsfield Unit (HU) is proportional to the degree of attenuation and approximately linear to the bone tissue density (Rho et al., 1995). The Young's Modulus can be determined from the apparent bone tissue density using a power relation found in Helgason et al. resulting in inhomogeneous material properties (Helgason et al., 2008). The relation between apparent bone density (ρ_{app}) and trabecular bone Young's Modulus (E) from Helgason et al. is:

$$E = 2017.3\rho_{app}^{2.46}$$

A disadvantage of using this method to determine the Young's Modulus is that high levels of radiation scatter and artefacts commonly exist in a CT scan (Razi et al., 2019). Artefacts can lead to an incorrect estimation of the bone density and hence material properties, particularly when low bone quality exists.

Alternatively homogeneous material properties can be considered for the trabecular and cortical bone. Maslov et al. conducted a finite element study of customised implants. It proposed a Young's Modulus of 10×10^3 MPa for cortical bone and an apparent density of 0.6×10^{-6} kg/mm³ for trabecular bone. Additionally, Maslov et al. gave a Young's Modulus of 1.1×10^5 MPa for titanium and 1×10^3 MPa for polyethylene (Maslov et al., 2019). The Young's Modulus of bone graft models have been reported as varying between 42 – 150 MPa (Totoribe et al., 2018). The elastic material properties of the graft have shown to vary substantially according to age, diagnosis, composition of trabecular and cortical bone and source of the bone graft (Voor et al. 2000).

2.2.3 Modelling Implant – Bone Interactions

The surface-surface contact between components controls the movement between two interfaces. In finite element studies involving implant-bone interactions, two types of contact are generally utilised; friction and bonded which allows for the level of osseointegration between implant and bone to be considered (Didier et al., 2020). Totoribe et al. developed a finite element model, focussing on bone grafts in the tibial bone. Within the model set-up, the interface between the bone and tibial component (titanium) was treated as friction with a coefficient of friction set to 0.2 (Totoribe et al., 2018). This coefficient of friction between titanium and bone is supported by Armentia et al (Armentia et al., 2020). Conflicting implant-bone surface contact was illustrated in Batista et al. and Didier et al., where all implant faces were bonded between components (Batista et al., 2017 & Didier et al., 2020).

2.2.4 Forces in the Hip Joint and Boundary Conditions

An intact hip joint will experience contact forces between the femoral head and the acetabulum. The influence of modelling the load accurately can influence the postoperative outcome of a CTAC as the outcome of this study may not be a true representation of the distribution of force within the screws. Knowledge of the biomechanics, particularly the hip joint forces in everyday life is essential for a successful study. For everyday life, walking is the most common exercise that is undertaken (Palmowski et al., 2021). Therefore, for the purpose of this study, the peak contact force between femoral head and the acetabulum during a complete gait cycle is under review.

In vivo studies have been performed determining the hip joint forces during everyday activities and collated in a database (Orthoload). The hip joint contact forces have been reported to vary between 209% body weight (BW) and 301% BW (Damm et al., 2015) with an average peak contact force of 253% BW (Figure 2.3) during a complete walking gait cycle. The direction of the peak contact can be represented in the x, y and z components acting on the femoral head. The peak contact force on the hip joint during a complete gait cycle is supported by Palmowski et al. that found a resultant contact force of 300.1 (\pm 38.4)% BW (Palmowski et al., 2021).

Figure removed due to copyright restriction

Figure 2.3: Hip joint contact forces during walking (Damm et al., 2015)

3 Project Methodology

3.1 Project Plan

The project plan can be summarised by a four-step process (Figure 3.1) to achieve the project aims. The development of the finite element model begun with the model set up in Simpleware ScanIP where the mesh was generated and material properties assigned to each of the components. Following, the components were imported into Abaqus to set-up the finite element model including the surface interactions between components, defining the applied load to the model and boundary conditions. The simulation was run where the force in each screw was extracted from Abaqus and the data analysed through MATLAB. These three steps were repeated for the different trial groups which will be further discussed, and all of the data was interpreted in MATLAB to observe the results.

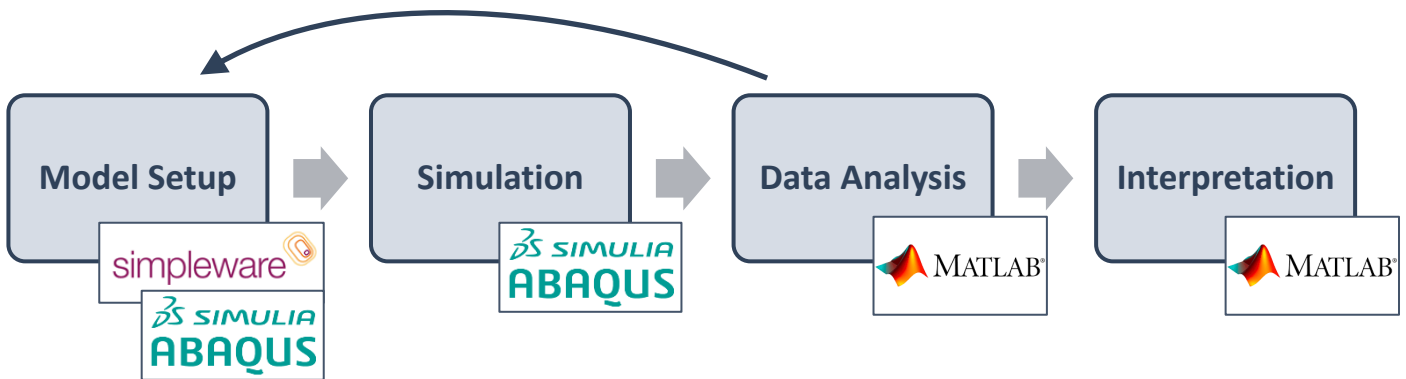


Figure 3.1: Project Plan

3.2 The Finite Element Model

Finite element analysis was the main tool that was utilised to achieve the project aims. To set-up the model, each component needs to be modelled, mesh generated and material properties assigned. Furthermore, the surface-surface contact between components, boundary conditions and applied load needs to be considered.

3.2.1 Pelvis and Custom Triflange Acetabular Cup

Modern imaging techniques such as magnetic resonance imaging (MRI) or computed tomography (CT) scans allow for biological structures to be reproduced digitally (Maslov et al., 2019). Simpleware ScanIP provides the ability to construct three-dimensional models from an image such as an MRI or CT scan. The bone geometry was segmented using algorithms to create the initial model. The segmented pelvis from the CT scan (Figure 3.2 – left) was previously developed and provided in the initial stages of the project. In addition to the pelvis, the custom triflange acetabular component (Figure 3.2 – right) specific to the patient was modelled and provided by OSSIS. The resulting three-dimensional model can be utilised for the FEA.



Figure 3.2: Computed Tomography scan of the patient (left) and constructed pelvis (pink) and implant (blue) from CT scan (right)

3.2.2 Proposed Screw Orientation

In addition to providing the computer-generated model of the pelvis and patient specific implant, OSSIS proposed a screw orientation that was used to fixate the implant to the pelvis (Figure 3.3). A total of 7 screws of varying length were modelled with each assigned a number. The length of screws can be found in Appendix II where screw no. 7 is the longest (measuring 59mm) and screw no. 5 is the shortest (measuring 22mm).

3.2.3 Components

For any THA that is being treated using a CTAC, there are generally six components that are utilised during surgery. Therefore, there are six components that were modelled to be able to accurately determine the force distribution within the screws. Modelling of these components was completed in SimpleWare ScanIP prior to the commencement of this project. The six components that the assembly (Figure 3.3) consists of are:

- (1) **Femoral head (grey)** – the femoral head provides the surface to apply the load to since it is the component that is attached to the femur.
- (2) **Polyethylene liner (orange)** – the polyethylene liner sits between the femoral head the CTAC and assists with stability, maximise range of movement and offset (Berend et al., 2018).
- (3) **CTAC (blue)** – the CTAC sits between the polyethylene liner and the pelvis to decrease component migration of the acetabular components.
- (4) **Screws (yellow)** – OSSIS has proposed a total of seven screws to fixate the implant to the bone. The screws are varying in length and position.

- (5) **Bone graft (light blue)** – the bone graft sits between the CTAC and the pelvis to aid in bone restoration and fixation of the CTAC to the pelvis.
- (6) **Pelvis (red)** – the pelvis can be observed to have significant deterioration as expected from the CT scan. The pelvis was assigned shell elements of constant thickness to represent cortical bone with a trabecular layer below.

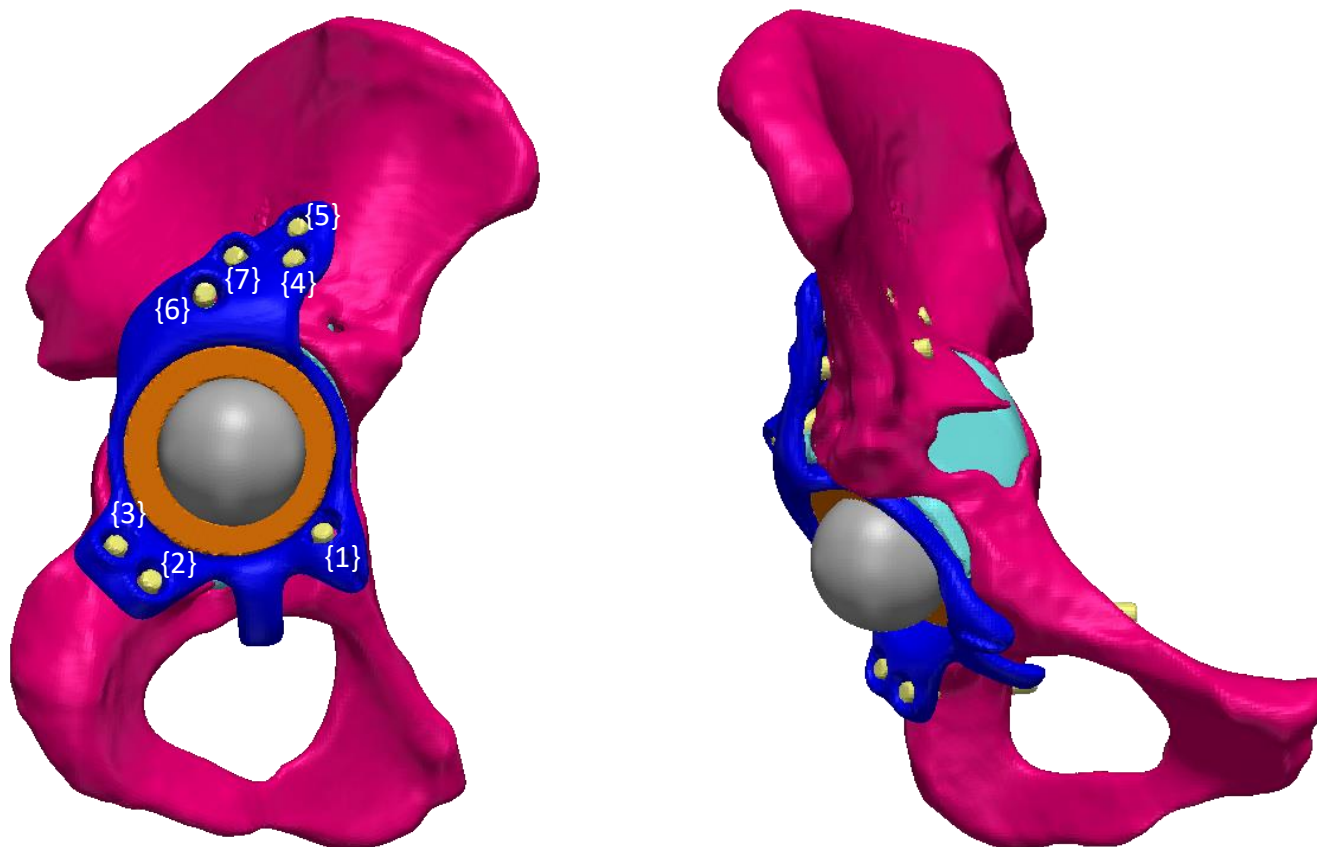


Figure 3.3: Components and screw orientation of the Finite Element Model

3.3 Mesh Generation

The volumetric finite element mesh was generated for each component in Simpleware Scan IP where the automated computed generated algorithm was utilised. All components were meshed with linear tetrahedral elements but varied in element edge length associated with the function and location of the component. The mesh for each of the screws and the CTAC were assigned to have a target minimum edge length of 0.68mm and a maximum edge length of 1.52mm. The screws and CTAC have been defined in the scope as the components of interest that data is gathered from, therefore, these components have been assigned a finer mesh. The mesh for the other 4 components (femoral head, polyethylene liner, bone graft and pelvis) were assigned to have a target minimum edge length of 0.96mm and a maximum edge length of 2.24mm to decrease the computational expense of the simulation. The options that are associated with each selection can be found in Appendix IV and the generated mesh for each component can be observed

in Figure 3.4. A localised mesh refinement was completed which involves decreasing the mesh density in the screws. Mesh is utilised to approximate the CAD geometry and to gain confidence of the accuracy of the mesh, the model was resolved with a finer mesh and the results compared. Performing a mesh refinement, particularly increasing the mesh within the screws to observe the effect on the force distribution will aid to validate the mesh chosen for the study.

3.3.1 Material Properties

The material properties (Young's Modulus and Poisson's Ratio) for each component were assigned in Simpleware Scan IP. The value assigned to each component (Table 3.1) for the two parameters were found from literature as discussed in chapter 2, section 2.2.2. Shell elements were set to model the cortical bone of the pelvis to replicate the structure of the bone. A constant thickness of 1mm for the shell elements was utilised which was adopted from previous studies in the Literature (Anderson et al., 2005). Additionally, a single modulus was utilised for trabecular bone due to the presence of artefacts in the CT scan provided. If the bone density was calculated from the attenuation in the CT scan, the large presence of artefacts would lead to an incorrect estimation of the Youngs Modulus. Utilising a single modulus for the trabecular bone also decreases the computational expense of the model. All material properties were considered to be isotropic and linear elastic.

Table 3.1: Material Properties

Table 3.1: Material Properties		
	Figure removed due to copyright restrictions	

[1] Maslov et al., 2019 [2] Helgason et al., 2007

3.3.2 Component Interactions

Assigning the surface-surface contact between components will impact the results. Two types of surface-surface contact were utilised in the finite element model. Contact with Coulomb friction was modelled for the CTAC-bone interface and the screws-bone interface with a coefficient of friction of 0.2 (Armentia et al., 2020). The contact between the other components at the interface (femoral head-liner, liner-CTAC, screws-CTAC and graft-pelvis) was assumed to be fully bonded with a tie constraint which does not allow for any movement between surfaces.

3.3.3 Applied Load

The applied force (Figure 3.4 – left) on the femoral head was two part; a nominal load perpendicular to the surface of the femoral head and another adopted from an Orthoload dataset. An initial nominal load of 100N for the first set of trial groups was selected to determine the distribution of this force within the seven screws with a nominal load applied.

Investigations into the forces within the hip joint was conducted in Chapter 2 which found a peak force on the femoral head during a complete gait cycle based on a percentage of body weight. It was found that the peak contact force on the femoral head during a gait cycle was 253% BW. The specific weight of the patient for this case was not given, therefore a generic weight of 80kg (784 N) was utilised. The two applied forces will exhibit an x, y and z component to be applied to the surface of the femoral head (Table 3.2).

Table 3.2: X, Y & Z components of applied force

Load	Magnitude (N)	F _x (N)	F _y (N)	F _z (N)
Nominal	100	79	25	56
Adopted from Orthoload	1984	774	127	1838

3.3.4 Boundary Conditions

The pelvis was rigidly fixed at the sacroiliac joint and the pubic symphysis (Figure 3.4 – right). The boundary condition was set by manually selecting the nodes at the sacroiliac joint and pubic symphysis as seen by the red nodes highlighted in Figure 3.4 and restraining the movement of those nodes to zero.

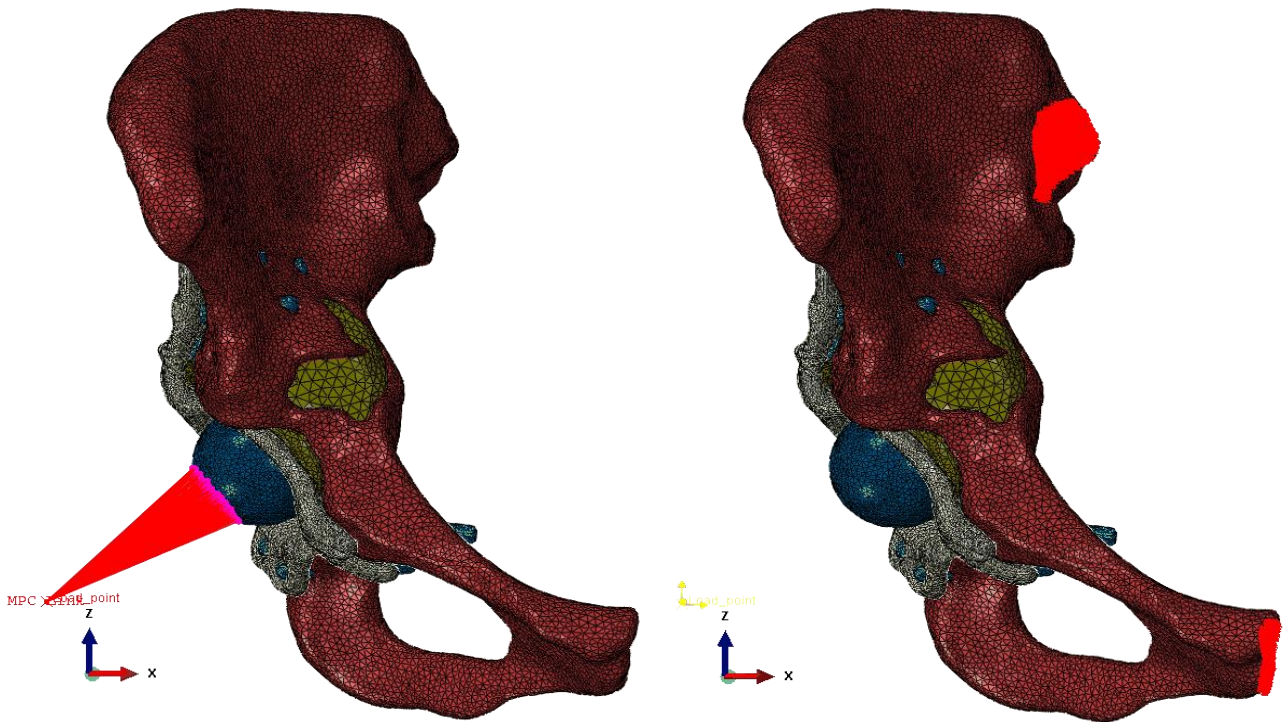


Figure 3.4: Load applied perpendicular to the surface of the femoral head (left) and boundary conditions (right)

3.4 Simulations

3.4.1 Achieving the Aim

To achieve the effect of screws not gaining fixation intraoperatively, this can be modelled by the screw being suppressed in Abaqus (which simulates removing the screw from the model). Therefore, a total of three different trial groups were conducted under the two different mechanical loadings.

- (1) **Trial Group 1** – All screws active.
- (2) **Trial Group 2** – Suppress one screw at a time starting with screw number 1 up to screw number 7. This gives a total number of simulations of 7.
- (3) **Trial Group 3** – Suppress two screws at a time with screws number 1 and 2, then numbers 1 and 3 etc. This gives a total number of simulations of 21.

The results from the three different trial groups were expected to show which screws are withstanding the most load, in addition to when certain screws fail, the effect of the load distribution on the remaining screws. The three trial groups were repeated twice, varying the applied load to the surface of the femoral head as discussed in section 3.3.3.

3.4.2 Graft Material Properties Verification Study

Verification studies are vital to ensure the FEA results are representing the load distribution that would occur in a human pelvis. A verification study was completed regarding the material properties of the bone

graft. Since, there is an assumption associated with selecting the graft material properties – particularly the Young’s Modulus – a study was performed altering this assigned value. Altering the Young’s Modulus of the bone graft, it is expected that the force transmitted into the screws would decrease as the Young’s Modulus increases as the bone graft would withstand more load. Completing this verification study will enhance the validity of the results.

3.5 Data Analysis

The force that each screw exhibits while under load is measured using Abaqus. The normal force at each of the nodes within the screw is extracted from Abaqus using the report function after the simulation was complete. Using both excel and MATLAB, the total normal force in each screw was determined from the report file (using code found in Appendix V).

3.6 Mesh Refinement Study

To ensure an appropriate mesh has been set for the study, it is good practice to perform a mesh refinement study. A mesh refinement study involves simulating the same problem with a finer mesh. For this study, the normal force in the screws was under investigation, therefore, it is only necessary to increase the mesh within the screws. The mesh in the screws was increased to exhibit a target minimum edge length of 0.37mm and a maximum edge length of 1.39mm. This increased the number of elements within each screw. Two simulations were run, the first being with the mesh assigned as outlined in Section 3.3 and

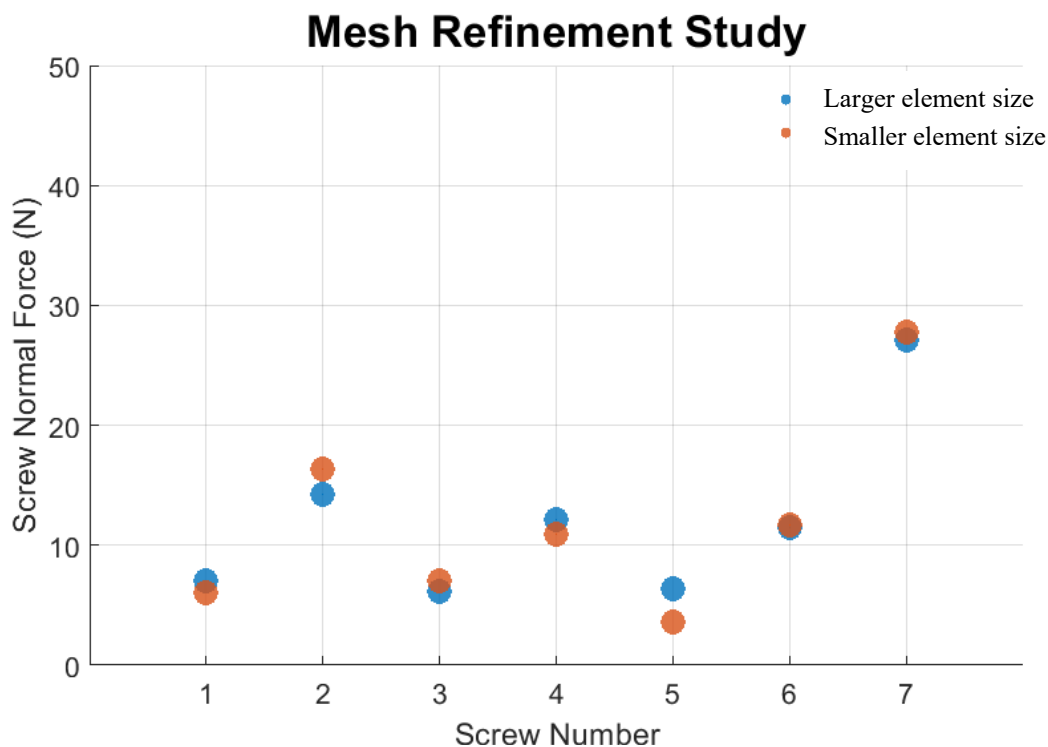


Figure 3.5: Mesh refinement under nominal load

another where the mesh was increased within the screws. Both simulations had all screws active for under the mechanical condition of applying the nominal load perpendicular to the femoral head (Figure 3.5).

The results produced from the mesh refinement study with a nominal load applied to the surface of the femoral head can conclude that the larger element size of the mesh generated in the screws is a good representation of the model. Under the nominal load, the load transmitted into each screw was adequately consistent for both meshes of the screws. Performing the mesh refinement study under the nominal load investigated in this study has enable the verification of the larger element size of the mesh in the screws which gives confidence regarding the mesh assignment.

4 Normal Force Distribution with Nominal Load

The normal force in each screw was extracted out of Abaqus for three initial trial groups when a nominal load was applied perpendicular to the surface of the femoral head. To observe the effect on the force distribution when a failure mechanism occurs in the screws, the second trial group was set-up to suppress one screw at a time. Furthermore, the third trial group was set-up to suppress two screws at a time under the initial nominal load.

4.1 Results

4.1.1 1st Trial Group: All Screws Active

The total normal force when all screws are active (Figure 4.1) represents the force distribution (in Newtons) within the seven screws when all gain fixation into the host bone. The sum of the forces (summing x, y and z components) within the screws was calculated to be 51.54 N which represents the percentage of applied load that the screws are withstanding. Therefore, within the seven screws, 51.54% of the load is transferred into the screws and the remaining 48.46% into the other components (pelvis, bone graft and custom triflange implant).

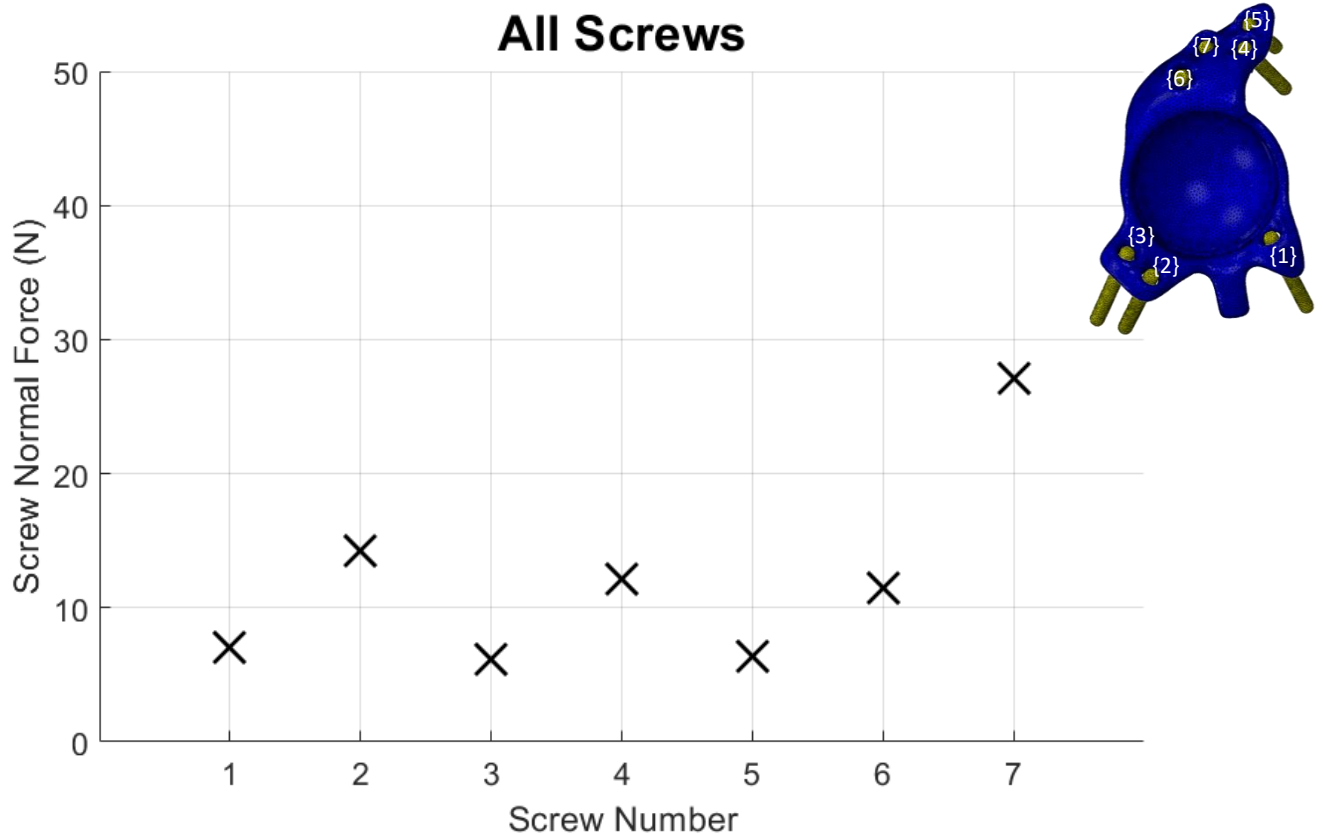


Figure 4.1: Force distribution when all screws active for first trial group

4.1.2 2nd Trial Group: Suppress 1 Screw at a Time

The second trial group consisted of suppressing one screw at a time to observe the effect on the force distribution when screws do not gain fixation intraoperatively (Figure 4.2 – the different colours represent the force transmitted into each screw for each of the trails). Comparison can be made from the results comparing the force variation to the force when all screws were active (the ‘X’ label for each screw). The total force transmitted into the screws for each simulation was calculated which produced an average of 49.25 N transmitted into the screws under these conditions. Therefore, an average of 49.25% of the applied force to the femoral head was transmitted into the screws when one screw does not gain fixation into the host bone. This increases the remaining load being transmitted into the other components.

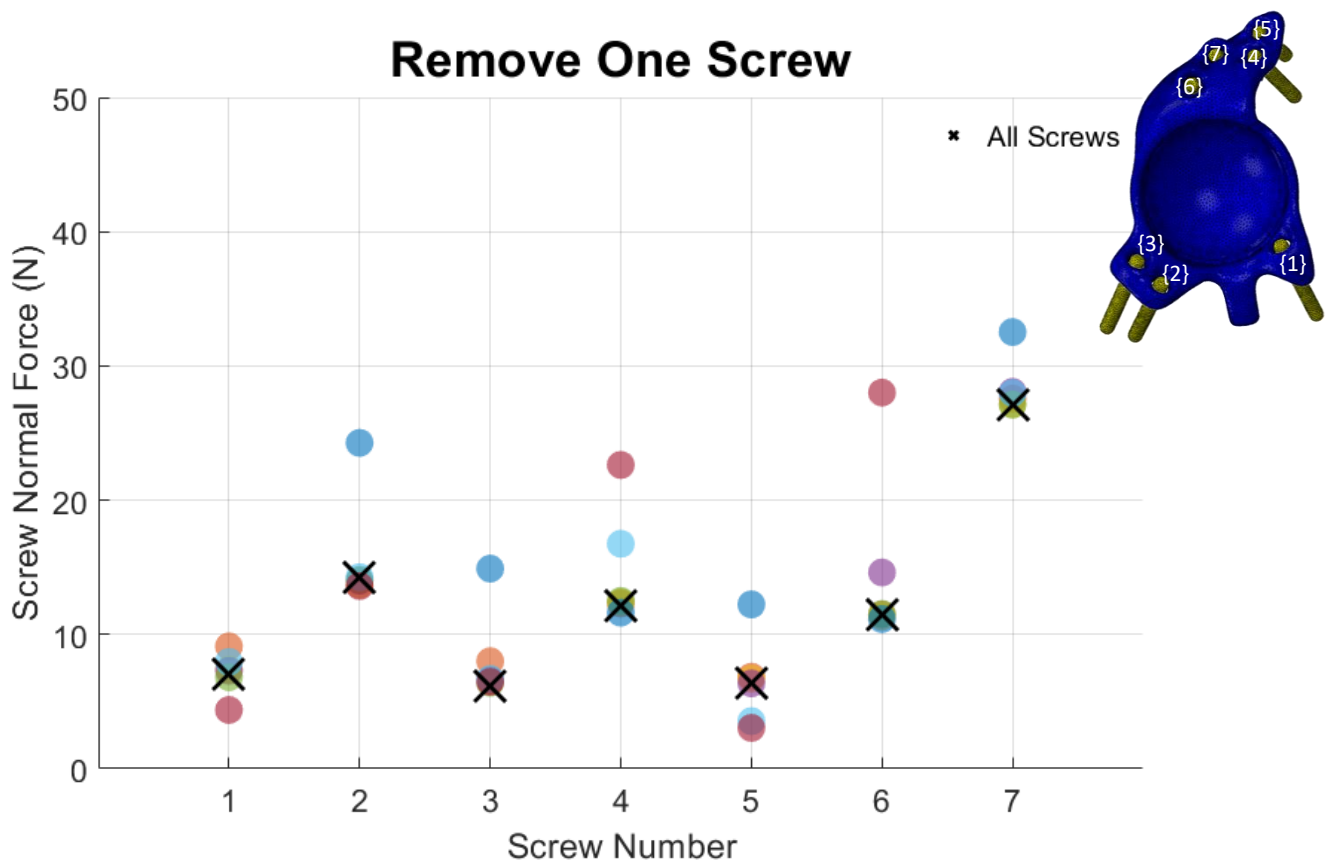


Figure 4.2: Force distribution in the screws for second trial group

4.1.3 3rd Trial Group: Suppress 2 Screws at a Time

The third trial group consisted of suppressing two screws at a time for a total of 21 trials. The effect on the force distribution in each screw (Figure 4.3) shows the range of force that is transferred into the screw when two screws do not gain fixation into the host bone. The total force within all the screws was calculated for each trial and an average of 46.06 N was transmitted into the screws. Therefore, on average, when two screws do not gain fixation into the host bone 46.06% of the applied load was being transmitted into the screws.

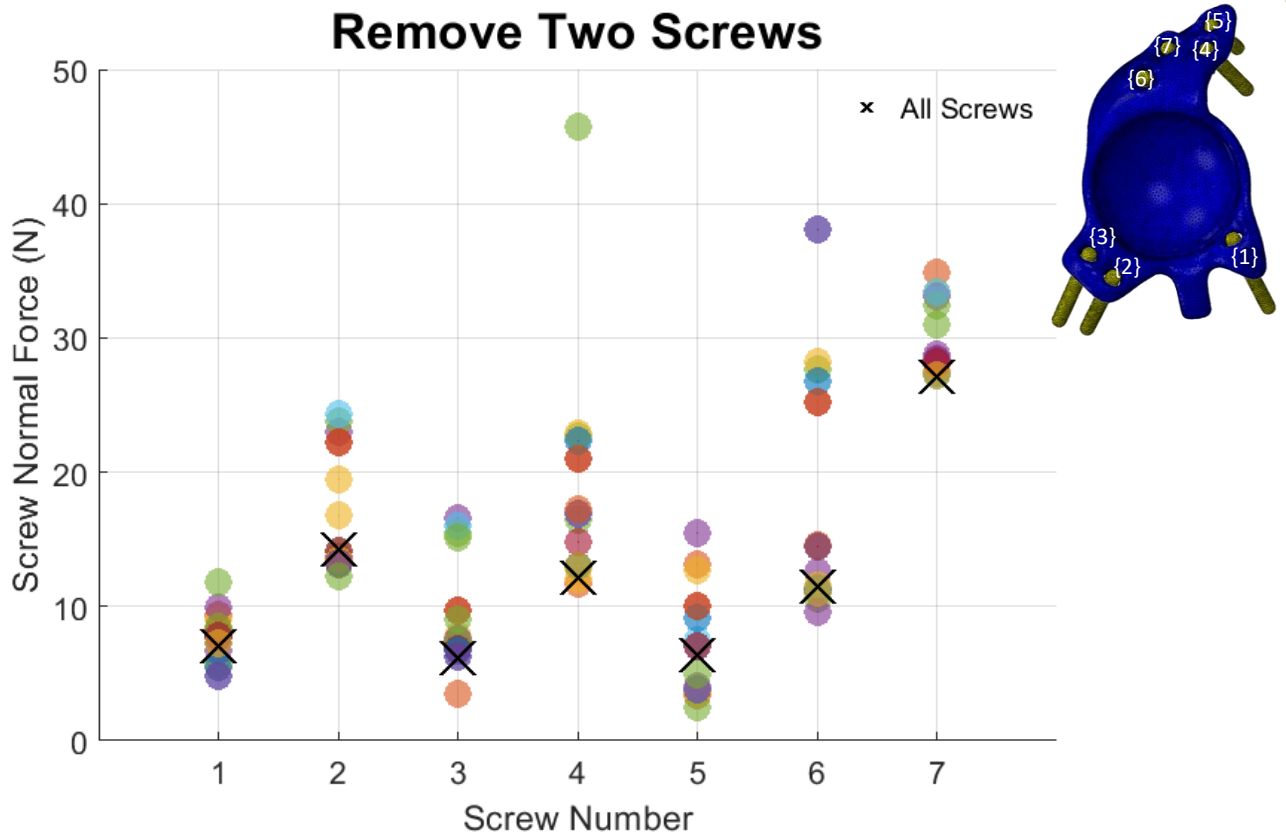


Figure 4.3: Force distribution in the screws for third trial group

4.2 Discussion

Under a nominal load applied perpendicular to the surface of the femoral head, the resulting force distribution in the screws (Figure 4.1, Figure 4.2 & Figure 4.3) utilised to fixate the cup vary depending on which screws are suppressed. When all screws gain fixation into the pelvis (when all screws are active), the largest amount of load was transmitted into screw number 7 which is the longest screw. Currently, inadequate component fixation is predominately due to loss of ischial fixation (Holt and Dennis, 2004). Ischial fixation is determined by screws number 2 and 3 in relation to the screw orientation of this study. When all screws are active, the force transmitted into screw number 2 is the second highest load and screw number 3 the lowest. Therefore, from the initial trail there is indication that screws number 2 and 7 are two critical screws to reduce the risk of component migration. This is supported by the force per millimetre within each screw (Figure 4.4) where the force transmitted into screw number 2 is the largest per millimetre of length and screw number 7 is the second largest.

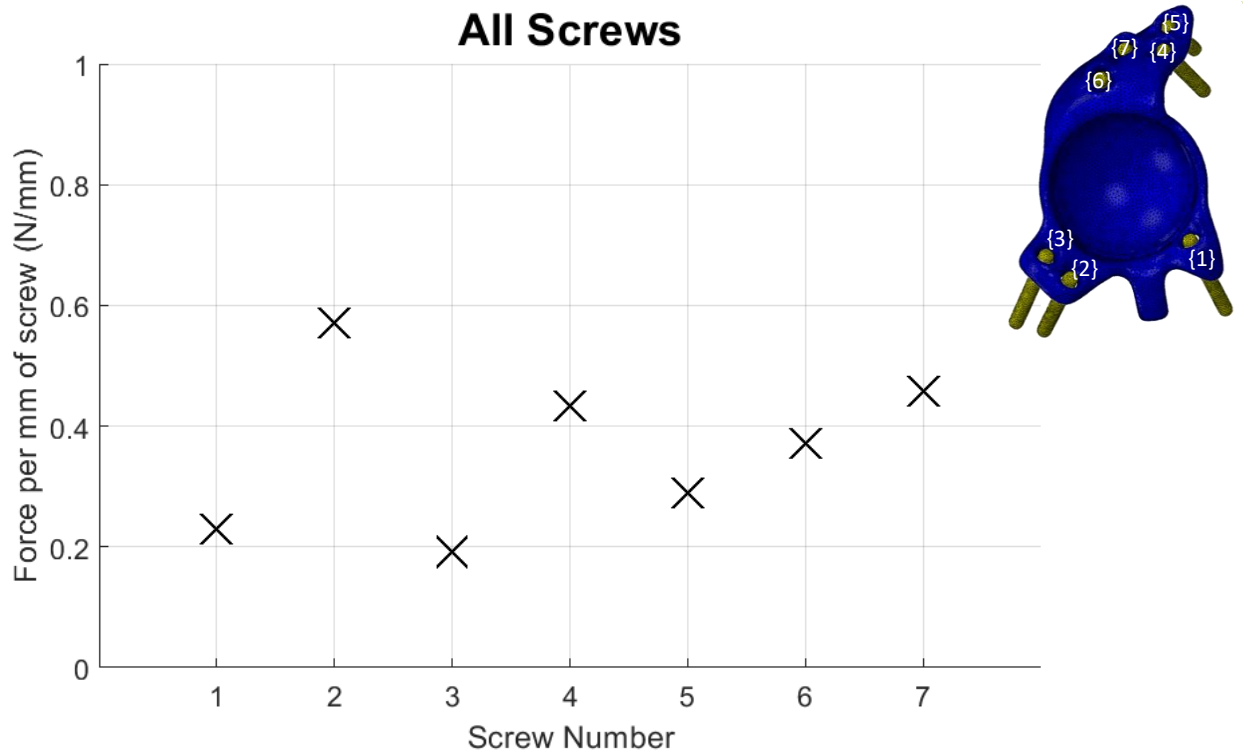


Figure 4.4: Force per millimetre of length when all screws were active

The second trial group (Figure 4.2) showed the variation in the screws when one screw does not gain fixation. The resultant data from this trial group recognises the force distribution in the screws when one screw does not withstand any force. The largest variations in force exists in screw number 2, screw number 4 and screw number 6 which occurs when screw number 1 (Figure 4.5 – left) and screw number 7 (Figure 4.5 – right) are suppressed respectively. A large increase in force within a screw is not desirable as it increases the risk of screw failure, particularly fracture. Therefore, further to screws number 2 and 7 being critical, from the second group of trials, it can be concluded that screw number 1 is also critical to increase fixation of the implant to the pelvis. Additionally, it supports the results from the 1st trial group to provide evidence screw number 7 is critical to ensure primary fixation.

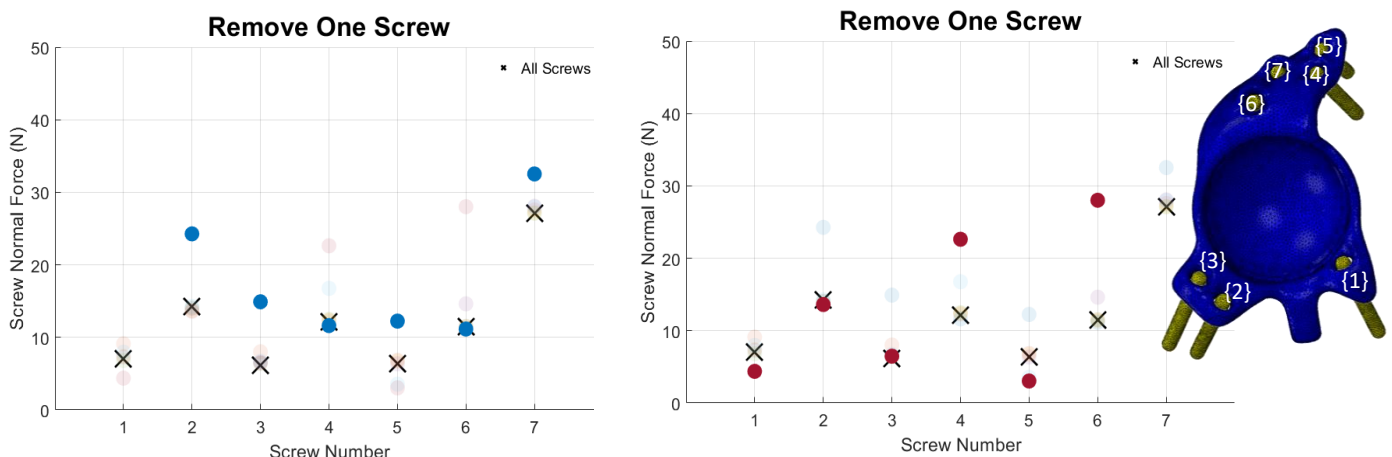


Figure 4.5: Screw number 1 suppressed (left) & screw number 7 suppressed (right)

The third trial group (Figure 4.3) showed the mechanical environment within the screws when two screws were suppressed at a time. The variation of forces, particularly in screws number 4 and 6, is much larger than the second trial group. The large force increase within screw number 4, resulted from suppressing screws number 6 and 7 (Figure 4.6 – left). Therefore, if screws number 6 and 7 were not able to gain fixation intraoperatively, screw number 4 would have a significant increased risk of screw failure (the screw itself). The large increase in force within screw number 4 is significantly larger (approximately double) compared to only suppressing screw number 7 (Figure 4.5 – right). This gives enough evidence to suggest that screw number 6 is also crucial to gain fixation to avoid the significant increase of force transmitted into screw number 4. Similarly, when screws number 4 and 7 are suppressed (Figure 4.6 – right), screw number 6 has a significant increase of screw failure. However, there is not enough evidence to suggest that suppressing screws number 4 and 7, the increase of force in screw number 6 is due to suppressing the combination of screws number 4 and 7. The increase in force transmitted into screw number 6 is consistent when only screw number 7 was suppressed from the first trial group. This evidence suggests that the addition of suppressing screw number 4 does not alter the force distribution within the remaining screws. Therefore, from the third trial group, it can be concluded that an additional screw number 6 is critical to avoid screw failure.

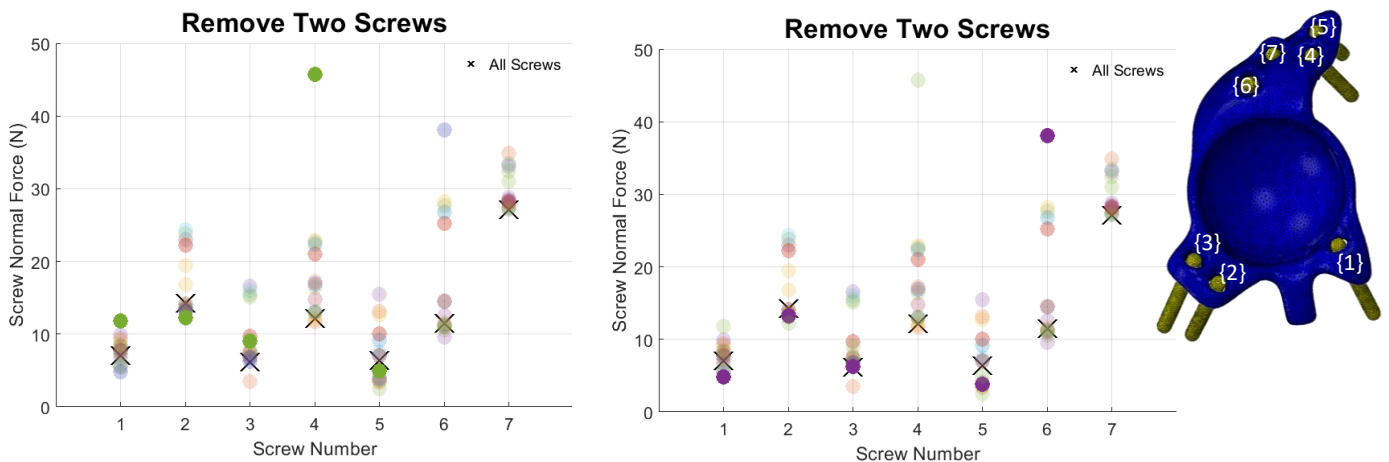


Figure 4.6: Screws number 6 and 7 suppressed (left) and screws number 4 and 7 suppressed (right)

The second trial group of suppressing one screw at a time provided evidence that individually screws number 1 and 7 are crucial to minimise a large force increase within the remaining screws (Figure 4.5). Suppressing both screws number 1 and 7 simultaneously in the third trial group (Figure 4.7 – left) increases the force transmitted into screws number 2, 4 and 6 which is consistent with suppressing each of these screws individually. Compared to other trails (Figure 4.6), the increase in force transmitted into the remaining screws isn't as extreme but would still increase the risk of screw fracture if both screws do not gain fixation intraoperatively.

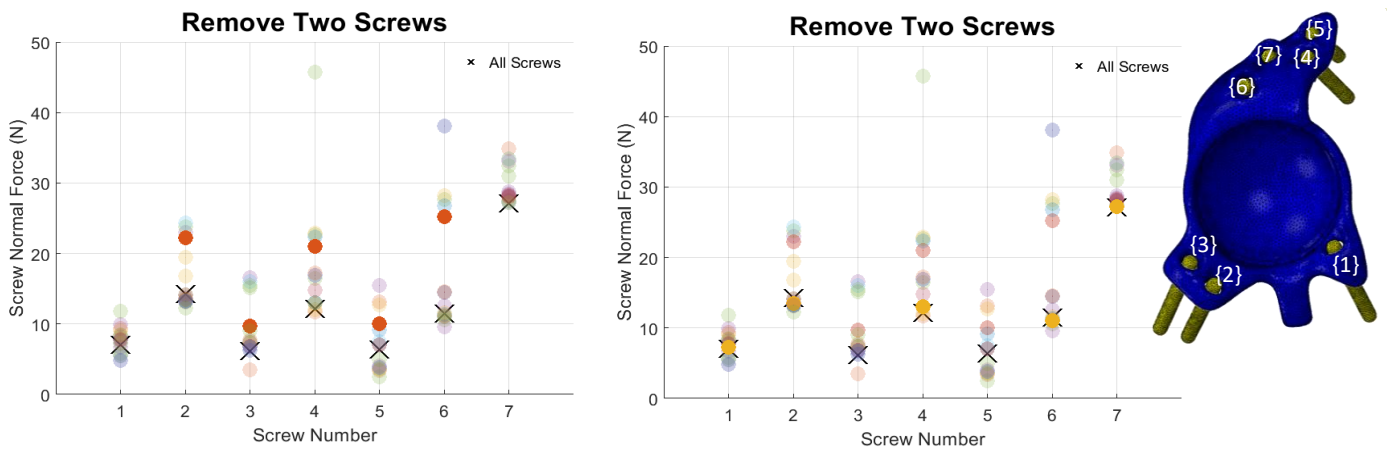


Figure 4.7: Screws number 1 and 7 suppressed (left) and screws number 3 and 5 suppressed (right)

From the three initial trial groups when a nominal load of 100 N is applied perpendicular to the femoral head, screws number 1, 2, 6 and 7 are the most vital screws to gain fixation intraoperatively. If any, or a combination of these screws were to not gain fixation into the pelvis, there is a significant risk of screw fracture in at least one of the remaining screws. This leads to a significant increase in implant migration and hence failure. In each of the figures, a comparison can be made to the force when all screws are active (when all screws gain fixation into the host bone). This comparison can help understand the mechanical environment within the screws suppressing one and then two at a time. In the third trial group, when screws number 3 and 5 were suppressed, there was no variation in the remaining screws (yellow marker: Figure 4.7 - right) compared to when all screws were active ('x' marker: Figure 4.7 - right). Since screws number 3 and 5 have not provided evidence to be critical to avoid inadequate primary fixation of the implant. The results provide high confidence that screws number 3 and 5 are the least critical screws to gain fixation intraoperatively.

There is evidence to be able to suggest to surgeons in the perioperative plan which screws are most vital to gain fixation intraoperatively under these mechanical conditions. Screw number 1 is vital to obtain both primary stability and pubic fixation. Within the ischial region of the CTAC, screw number 2 is more vital to gain fixation compared to screw number 3. Similarly the evidence shows, in the ilial region, screws number 4, 6 and 7 are crucial to increase the primary stability of the implant. Therefore, if any screws were disregarded in the perioperative plan, screws 3 and 5 could be removed under the nominal load.

When all screws were active, the load transmitted into the screws was found to be 51.54% of the applied load. This load that was transmitted into the screws decreased when screws were suppressed. Suppressing one screw at a time resulted in the screws withstanding an average of 49.25% of the applied load and suppressing two screws at a time resulted in an average of 46.06% of the applied load. Therefore, when screws do not gain fixation intraoperatively, there is a trend to suggest that the load transmitted into the other components (particularly the pelvis and graft) is higher. With an already fragile bone from poor bone

quality, more load transmitted into the pelvis is not desirable as it has the potential to further deteriorate the bone.

5 Normal Force Distribution during a Complete Gait Cycle

The load applied to the surface of the femoral head was altered to represent the peak contact force on the femoral head during a complete gait cycle. The applied load was adopted from Damm et al. with a maximum contact force of 253% of the patient's body weight (Damm et al., 2015). For a generalisation of an individual's weight to be 80kg, the peak contact force on the femoral head is 1984 N ($F_x = 774$ N, $F_y = 127$ N & $F_z = 1838$ N). Similarly with Chapter 4, three trial groups were conducted to observe the effect on the force distribution within the screws supressing one and then two at a time.

5.1 Results

5.1.1 1st Trial Group: All Screws Active

The total normal force within each screw represents the transmission of the applied force into the screws under the peak contact force (Figure 5.1). The sum of force transmitted into the screws was calculated to be 1558.5 N which is 78.5 % of the applied force. Therefore, 78.5 % of the peak contact force on the femoral head during a walking gait cycle is being transmitted into the screws under these conditions.

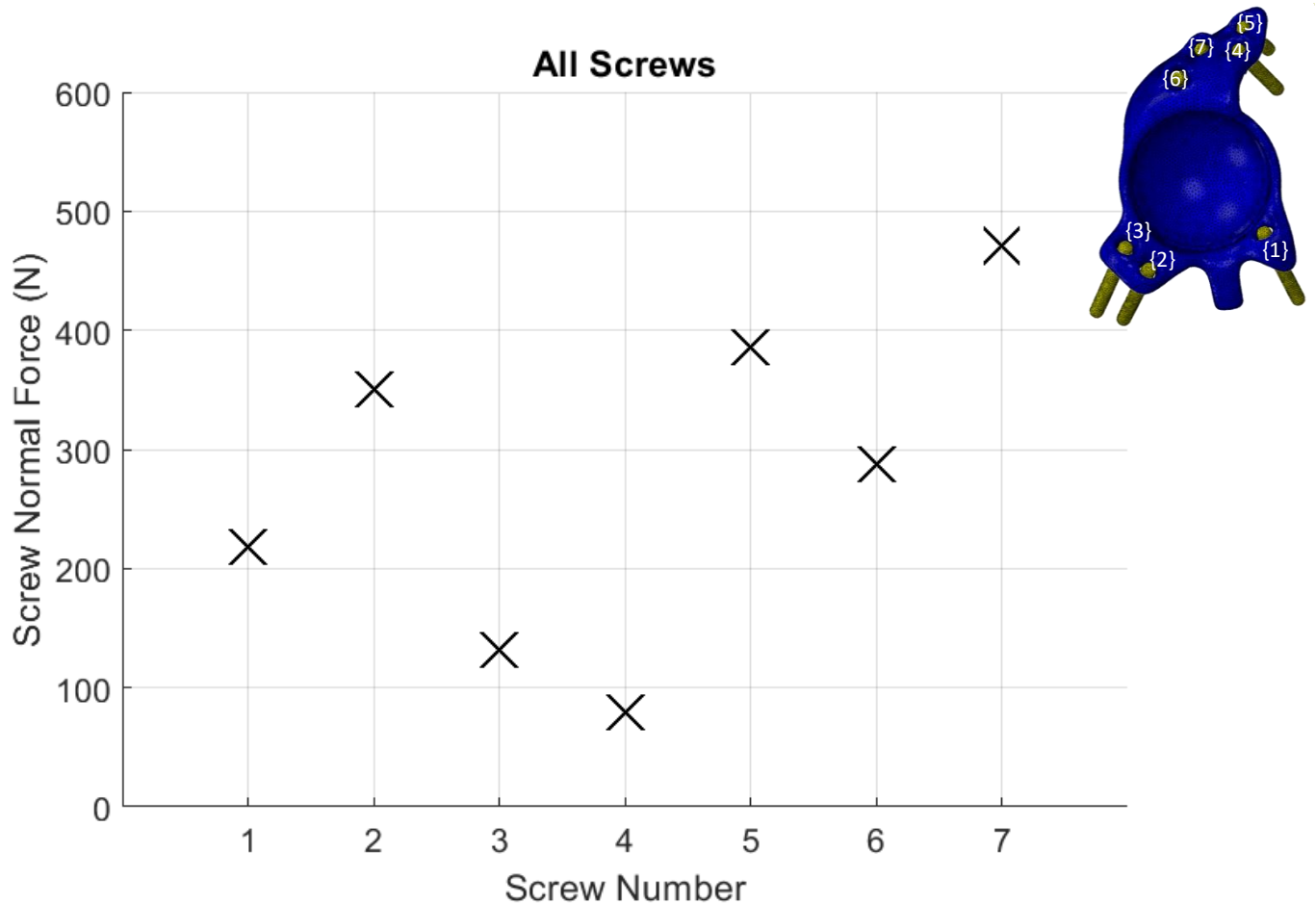


Figure 5.1: Force distribution when all screws are active under peak contact force

5.1.2 2nd Trial Group: Suppress 1 Screw at a Time

The second trial group consisted of suppressing one screw at a time to observe the effect on the force distribution within the screws (Figure 5.2). Under the conditions highlighted in Chapter 3 applying a peak contact force during a complete gait cycle to the femoral head, the average total force into the screws was calculated to be 1443 N. Suppressing one screw at a time simulates the mechanical environment in the system when a screw does not gain fixation either intraoperatively or postoperatively. When a screw does not gain fixation, an average of 72.7% of the peak contact force during a gait cycle is transmitted into the screws. The remaining load would be transmitted into the other components such as the graft and pelvis.

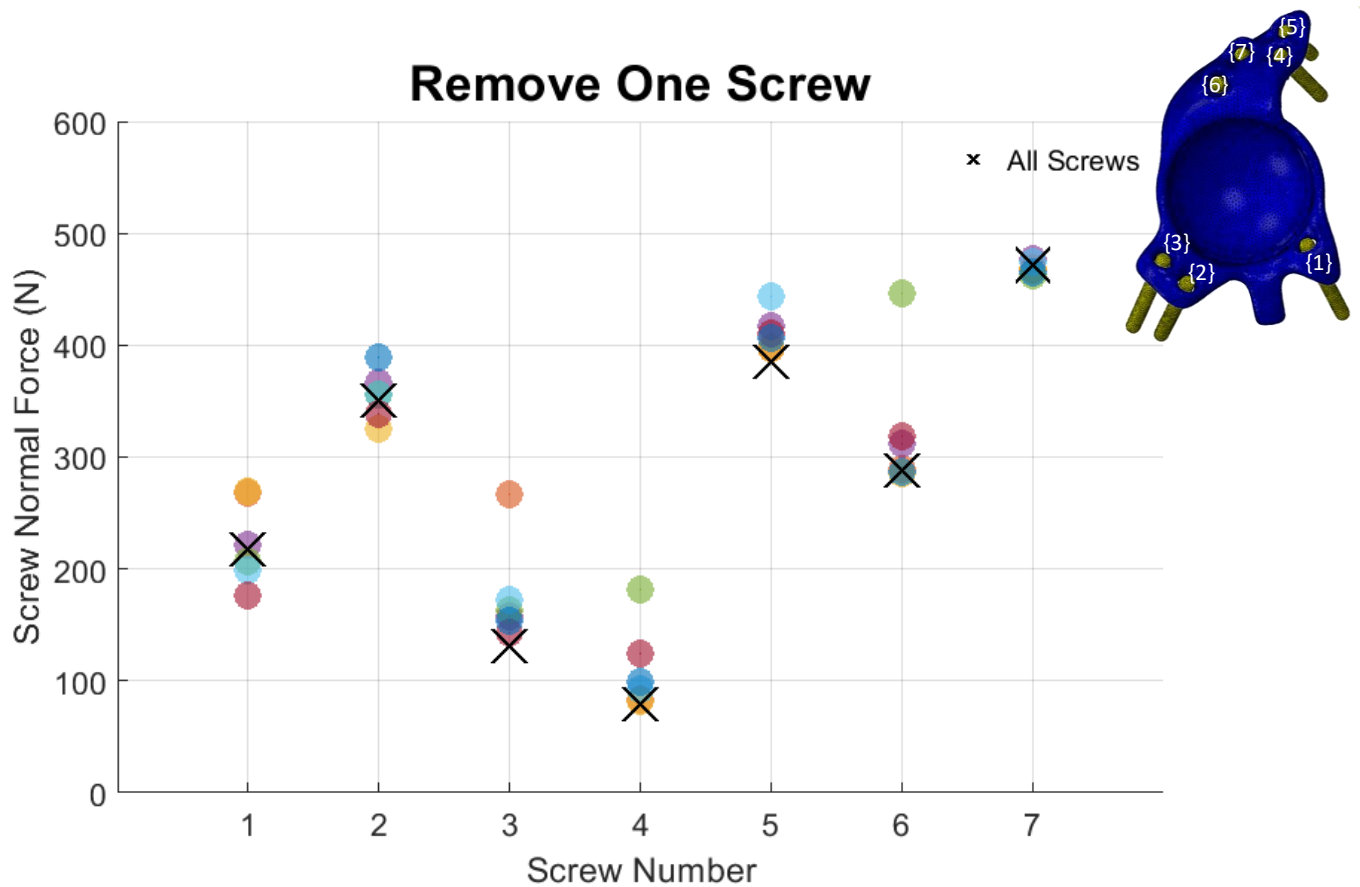


Figure 5.2: Force distribution suppressing one screw at a time under a peak contact force

5.1.3 3rd Trial Group: Suppress 2 Screws at a Time

Suppressing two screws at a time will enable the mechanical environment within the remaining screws to be observed under the peak contact force on the femoral head (Figure 5.3). The average load that is transmitted into the screws under these conditions was 1308 N which represents 67% of the applied load.

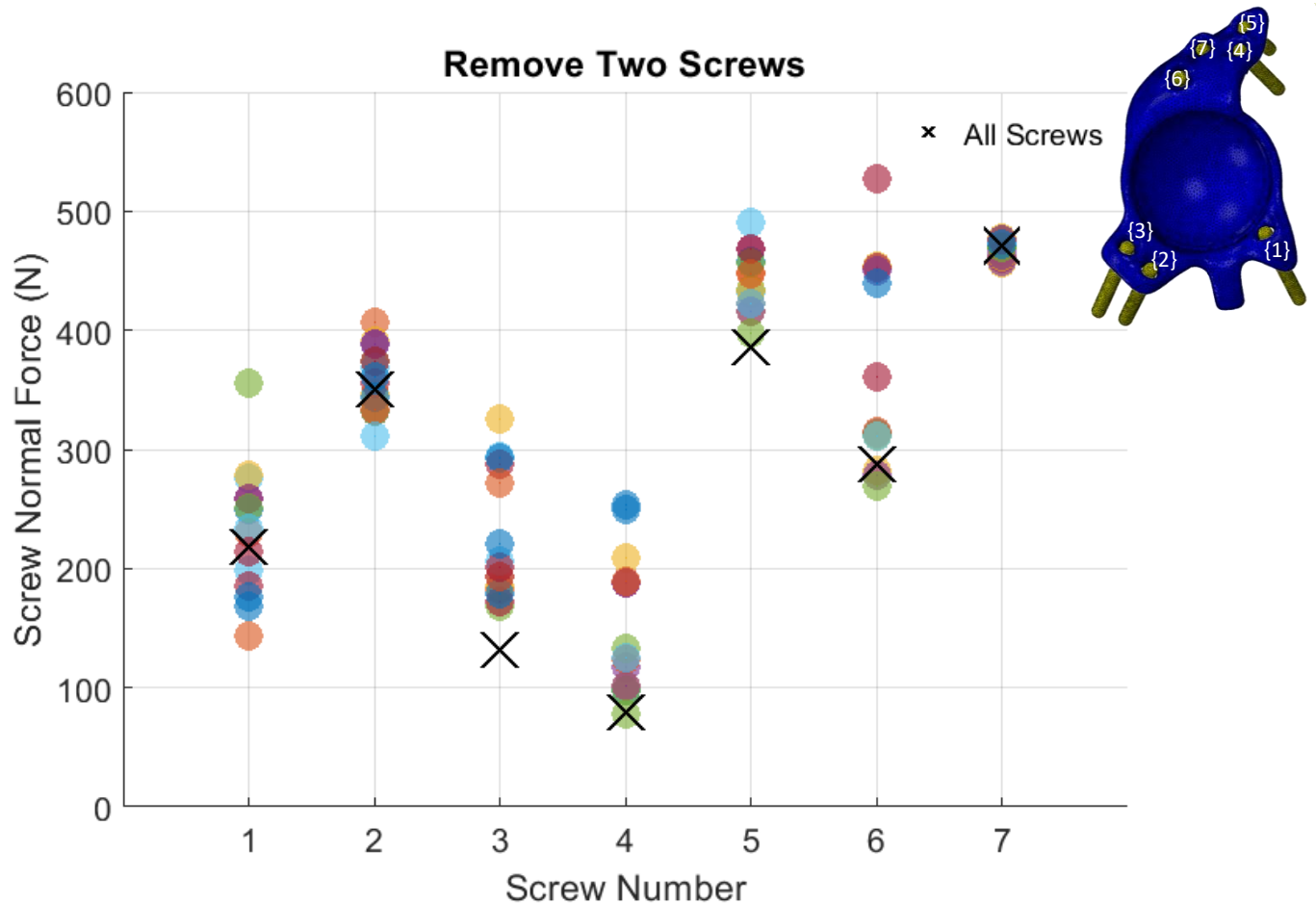


Figure 5.3: Force distribution suppressing two screws at a time under peak contact force

5.2 Discussion

The force distribution within the screws when all screws were active represents the mechanical environment within the cup at the peak contact force on the femoral head during a complete gait cycle. The force that would be transmitted into each screw can be observed (Figure 5.1) with screw number 4 exhibiting the least amount of force and screw number 7 the largest amount of force. The results show that the force transmitted into screws number 2 and 5 was also considerable. When all screws gain fixation into the pelvis intraoperatively, when a complete gait cycle is performed by the patient, at the peak contact force on the femoral head, 78.5% of the peak load is being transmitted into the screws. Screws number 2 and 5 are the shortest of the screws and screw number 7 is the longest (Appendix II). Therefore, under this peak load, there is an increased risk of screw fracture of screws number 2 and 5 since they are withstanding a considerable amount of load compared to the length of the screw. The force per millimetre of length transmitted into each screw (Figure 5.4) was calculated and supports that the force transmitted into screws number 2 and 5 are the largest per millimetre of length and could increase the risk of screw failure.

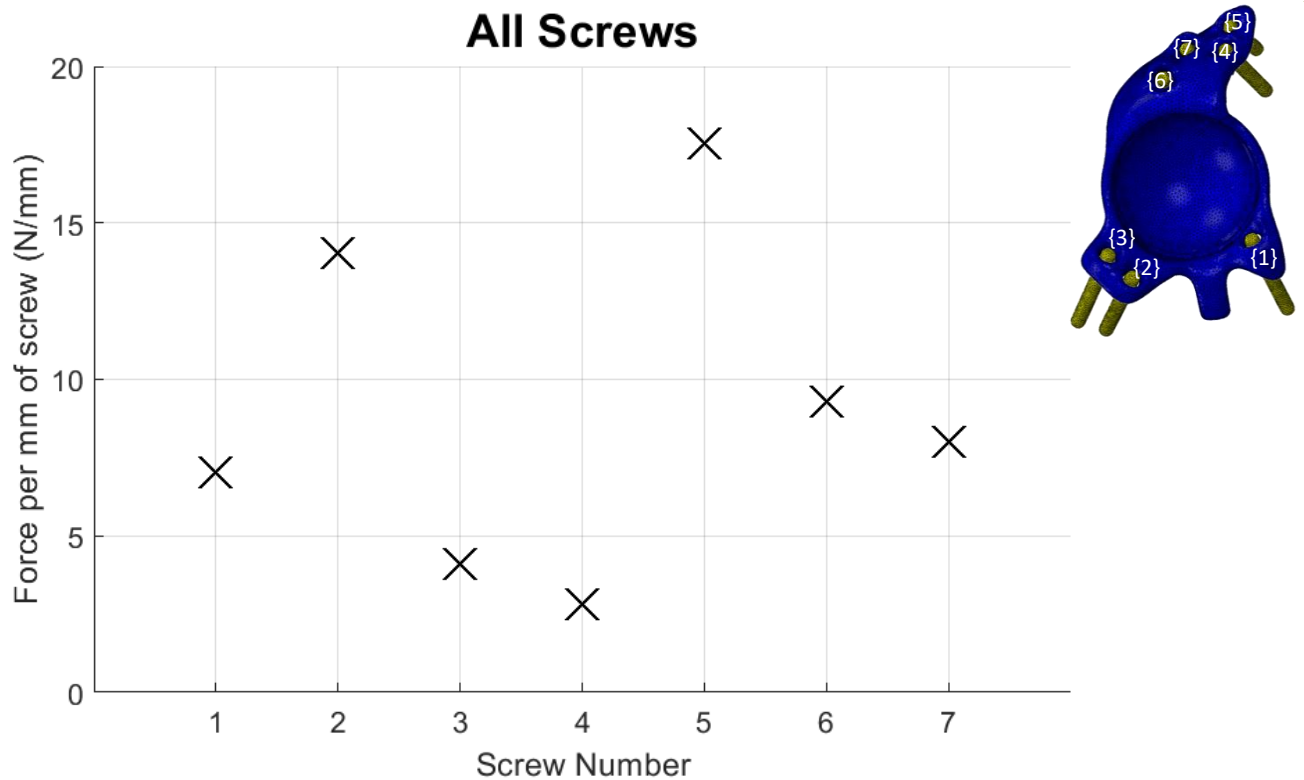


Figure 5.4: Force per mm within the screws

The second trial group consisted of suppressing one screw at a time which simulates when a screw does not gain fixation intraoperatively. An average of 72.7% of the applied load was transmitted into the screws under these conditions. Therefore, when one screw does not withstand any of the applied force, the force being distributed to the other components (pelvis and graft) increases. The largest variation in force was demonstrated in screws number 3 and 6 which occurs when screw number 2 (Figure 5.5 – left) and 5 (Figure 5.5 – right) are suppressed respectively. This provides evidence to suggest that screws number 2 and 5 are critical to gain fixation to decrease the risk of screw failure in screws number 3 and 6 which supports the results found from the first trial group.

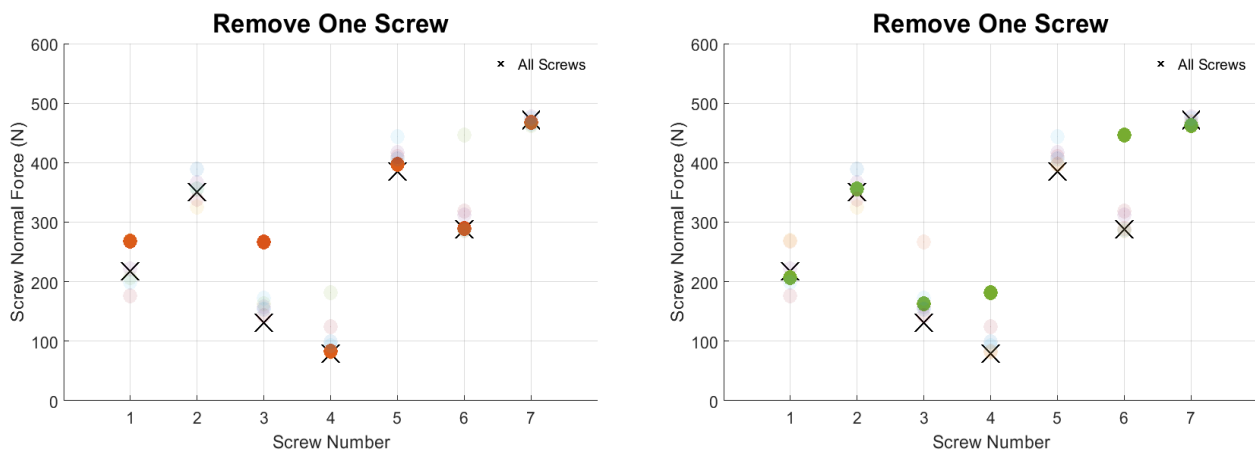


Figure 5.5: Screw no. 2 suppressed (left) & screw no. 5 suppressed (right)

The results from the second trial group showed the transmission of the force into screw number 4 was always the lowest. This supports the results from the first trial group, where screw number 4 had both the smallest force transmission and force per millimetre of length. When screw number 4 was suppressed, the variation of force transmission into the remaining screws compared to when all screws were active was minimal (Figure 5.6 – left). Therefore, when applying a peak contact force during a complete gait cycle to the femoral head, fixation of screw number 4 has minimal effect on the force distribution within the remaining screws and hence is the least critical to gain fixation if one screw was to be removed from the perioperative plan. Proving that suppressing screw number 4 does not have a significant impact on the force transmitted into the remaining screws gives an indication that the screw with the least force per millimetre of length (Figure 5.4) is the least critical screw to gain fixation and primary stability. Therefore, could be removed from the perioperative plan.

The third trial group consisted of suppressing two screws at a time. The average transmission of load into the screws, suppressing two screws at a time was calculated to be 67% of the applied load on the femoral head. Therefore, when two screws do not gain fixation intraoperatively, the transmission of the load into the screws decreases and hence transmitted into other components such as the pelvis or graft. From the second trial group, it could be observed that the screw with the smallest force per millimetre of length had the least impact on the force transmission into the remaining screws. This is supported when screws number 3 and 4 were suppressed (Figure 5.6 – right) as there isn't a considerable impact on the force transmitted into the remaining screws that would result a risk of screw failure.

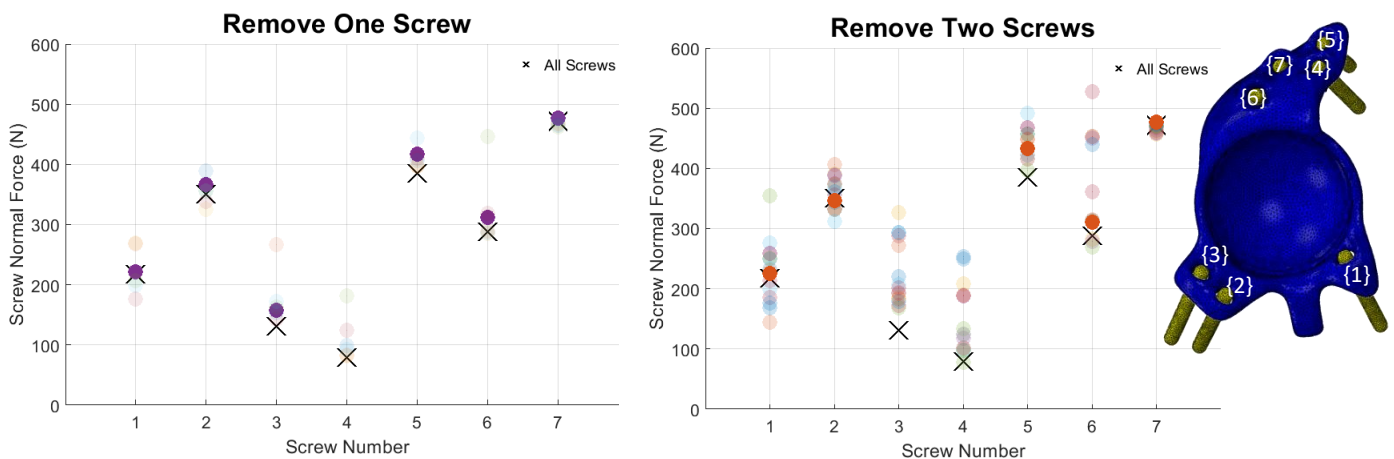


Figure 5.6: Screws number 4 suppressed (left) & screws number 3 & 4 suppressed (right)

From the results in the third trial group (Figure 5.3), a significant variation of force transmitted into screws number 1 and 6 exists. A large increase in force within screw number 1 is evident when screws number 2 and 3 are suppressed (Figure 5.7 – left) and a large increase within screw number 6 exists when screws number 4 and 5 are suppressed (Figure 5.7 – right). In all of the trials, when either screw number 2 or 5 were suppressed, there was a large variation in the force distribution in the remaining screws as screw

number 2 and 5 have been shown to be most critical to get fixation. Therefore, the combination with another screw does not conclude that the other screw is also crucial to reduce the risk of screw failure. Additionally, the simulation when screws number 3 and 4 were suppressed, the transmission of force into the remaining screws did not vary significantly compared to when all screws were active (Figure 5.6 - right). Therefore, from the third set of trial groups, it supports that screws number 2 and 5 are the critical screws to get fixation intraoperatively to reduce the risk of screw failure of one of the remaining screws.

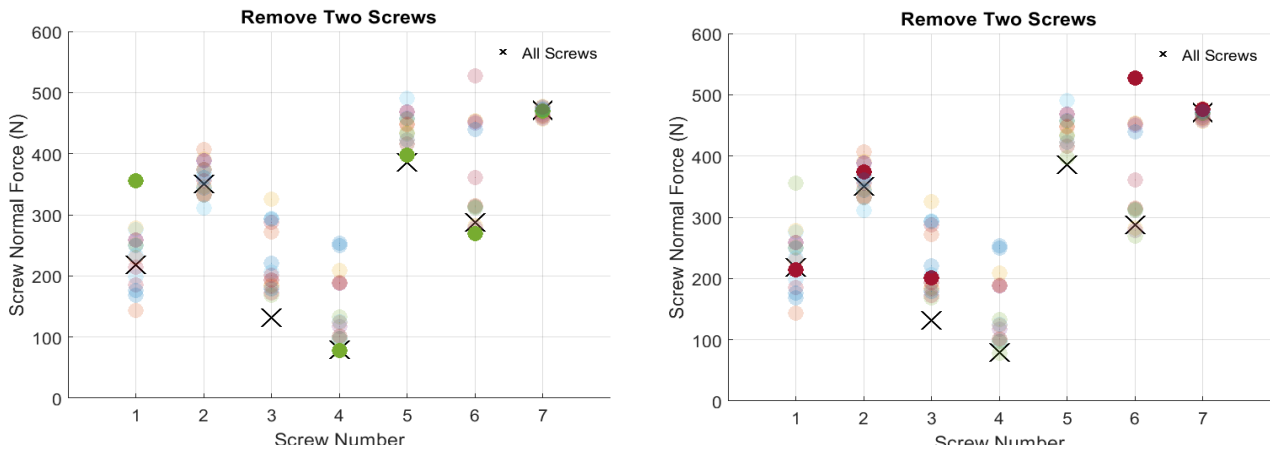


Figure 5.7: Screws number 2 & 3 suppressed (left) & screws number 4 & 5 suppressed (right)

Applying a different load to the femoral head will alter the force distribution within the screw significantly. The second mechanical environment for the study consisted of applying a load to simulate the peak contact force on the femoral head during a complete gait cycle. The peak force was found from literature with a magnitude of 253% of the patients body weight which is calculated to be 1984 N utilising a body weight of 80kg. When this load was applied, from the three trial groups, there is evidence to suggest that screws number 1, 3 and 4 are the least crucial to get fixation into the pelvis intraoperatively. When screws number 2, 5 and 7 do not gain fixation into the pelvis, the results show a significant increase in the force transmitted into at least one of the remaining screws. An increase in force transmitted into a screw, increases the risk of screw failure as there is an increased risk of screw fracture under the peak contact force. An increase in screw failure would affect the primary stability which could lead to a failed implant.

6 Graft Material Properties

Verification studies are essential to confirm the validity of the results found from the study. A verification study was completed investigating the effect of the force distribution in the screws by increasing the Young's Modulus of the bone graft. From literature, the material properties of a bone graft varied between 42 – 150 MPa (Totoribe et al., 2018). For a verification study of the model produced in this study, the Young's Modulus of the graft was varied between 5 MPa and 160 MPa to observe the effect on the force distribution within the screws. It is expected that increasing the Young's Modulus of the bone graft, a greater load would be transmitted into the bone graft and therefore, a decrease in load transmitted into the screws. The results from the verification study (Figure 6.1) showed that in every screw, as the Young's Modulus of the bone graft increased, the force within the screw decreased. Additionally, this suggests that the mechanical environment within the screws when the graft would fail is significantly higher especially in screw numbers 1 and 2. The highest rate of CTAC failure is predominately due to ischial pulloff (Holt and Dennis, 2004). Therefore, an increase in load within screw number 2 should be avoided as this screw would significantly impact the ischial fixation of the CTAC.

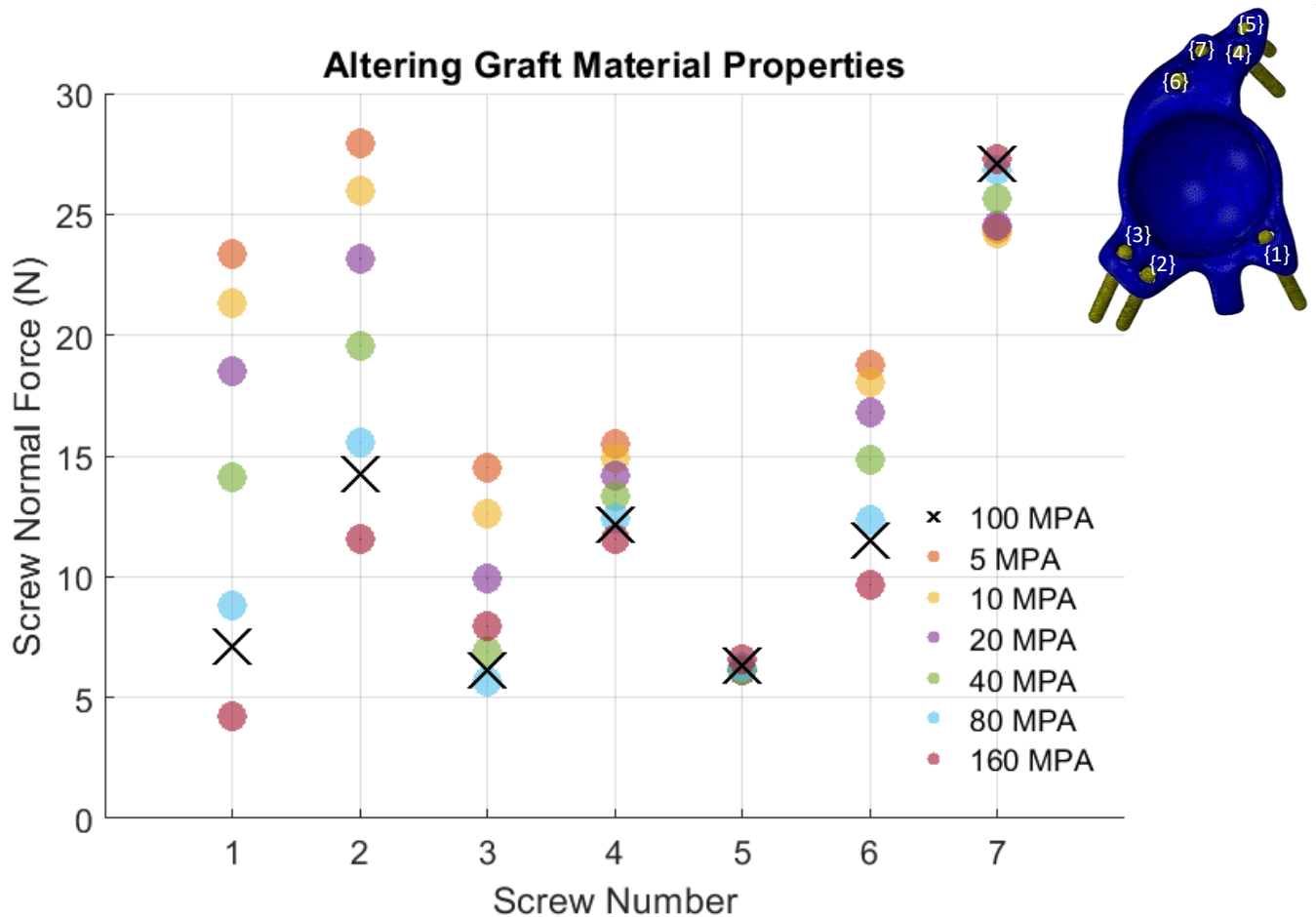


Figure 6.1: The effect on force distribution in screws when the graft material properties are changed

The overall force that is transmitted into the screws was calculated for each different Young's Modulus value assigned (Figure 6.2). The relationship between the total force within the screws at the Young's Modulus of the bone graft further confirms the validity of the model. As the Young's Modulus increases, the total force transmitted into the screws exponentially decays. If the graft failed to osseointegrate into the pelvis, this would be simulated with a Young's Modulus of 0 – 5 MPa. In this instance, the load transmitted into the screws is 100% of the applied load which would increase the risk of screw failure and hence component migration. As the graft osseointegrates into the pelvis, the Young's Modulus of the graft would increase and therefore, the load transmitted into the screws decreases.

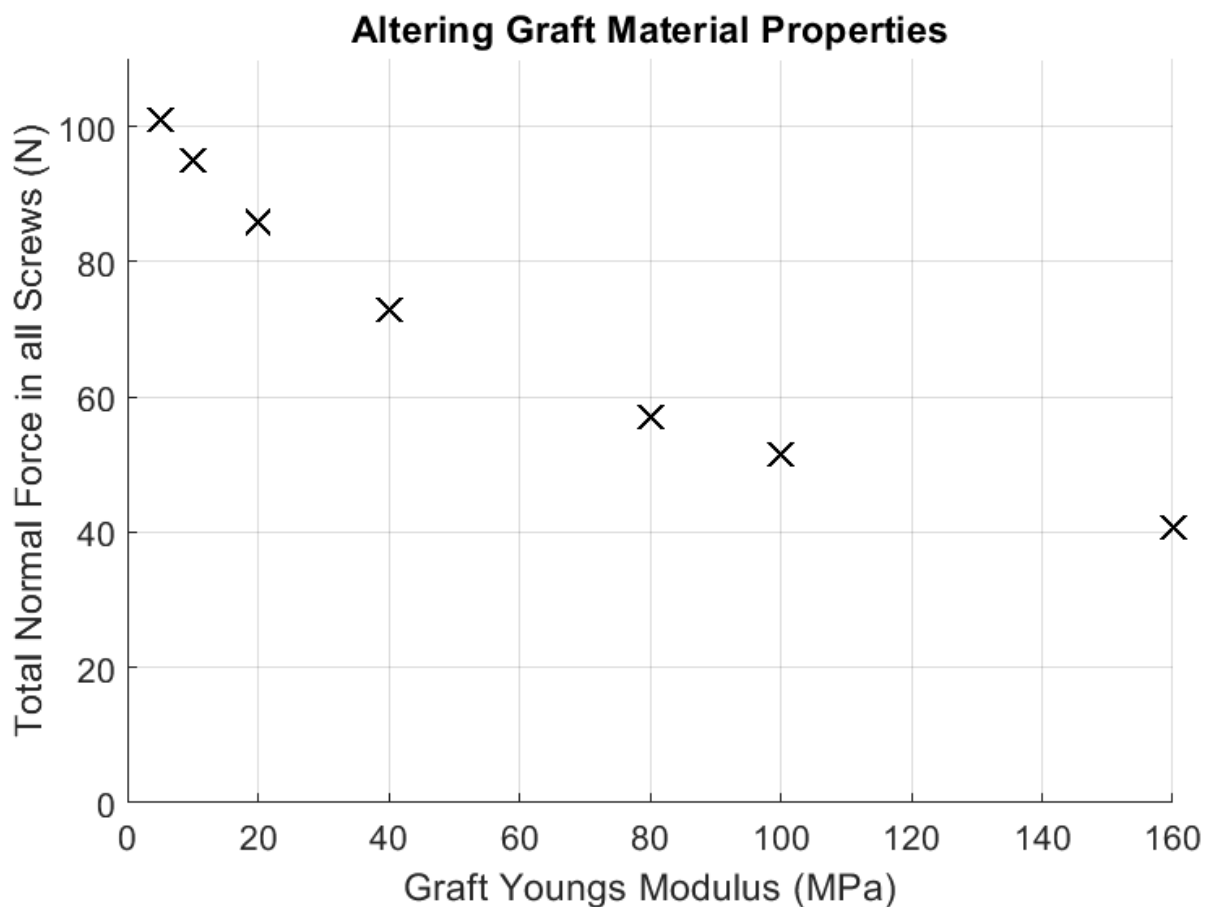


Figure 6.2: Relationship between graft Young's Modulus and total force within screws

7 Discussion, Limitations and Future Work

7.1 Discussion

The challenge of custom tri-flange acetabular components (CTACs) is to obtain primary fixation (immediately post-surgery), particularly when significant bone loss exists in the pelvis. To obtain fixation of the implant, a number of screws are utilised. Within Chapter 2, it was discovered that there is a gap in literature regarding the mechanical environment associated with the fixation methods utilised in a CTAC to obtain primary stability to the pelvis. In particular, it is unknown what screws are withstanding the most load and hence required to gain fixation intraoperatively to increase the chance of a successful total hip arthroplasty (THA). This study focussed on the force distribution within the screws under two load conditions. Varying the conditions within the pelvis can increase the understanding of the screw-bone interaction and which screws are required to gain fixation. In addition, there is limited research involving the appropriate orientation and number of screws that are required to obtain fixation and primary stability.

Chapters 4 and 5 presented the results found in the study under two different loading conditions. The first condition was applying a nominal load of 100 N perpendicular to the surface of the femoral head. The second condition was applying a peak contact force on the femoral head during a complete gait cycle adopted from Orthoload. The second condition would simulate the peak load that would be transmitted through the acetabulum during a complete gait cycle. Three sets of trial groups were completed for each condition, the first when all screws are active, the second suppressing one screw at a time and the third suppressing two screws at a time. The purpose of suppressing screws in the model was to observe the force distribution within the remaining screws to simulate the force transmission into the screws when particular screws do not gain fixation intraoperatively.

The results from Chapters 4 and 5 showed that the force within the screws varies significantly when different loads are applied to the surface of the femoral head. Chapter 4 concluded that screws number 1, 2, 6 and 7 are most vital to gain fixation intraoperatively to reduce the risk of screw failure within one of the remaining screws. Chapter 5 concluded that screws number 2, 5 and 7 are the most vital. Under both conditions, screw number 7 exhibited the largest amount of force and provide evidence to suggest that screw number 7 is critical to gain fixation under all applied load conditions. Additionally, under both conditions, the maximum force per millimetre of the length of the screw was found in screw number 2. However, the screw that least amount of force is transmitted into is not consistent under the two conditions. Therefore, there is evidence to suggest that the applied load on the femoral head has a considerable effect on the force distribution transmitted into the screws. For the purpose of this thesis, it is more important to discover the effect on the force distribution within the screws during a complete gait cycle as it is a better

representation of the force that would be present within the pelvis. From Figure 2.3, it can be observed that the contact force on the femoral head does not vary significantly and never would be as low as the nominal load of 100N during a gait cycle. Therefore, a recommendation will be performed only from the results found in Chapter 5.

Utilising more screws than necessary to ensure fixation of a CTAC can lead to further deterioration of the pelvis, especially if the implant fails. When an implant fails, all of the components and screws are removed, leaving holes in the bone and hence further deteriorating the bone. Therefore, the bone is weaker and can break through the screw holes easier under impact (Mathes, 2015). In a revision, new holes are required for the screws to gain fixation into the pelvis which can lead to further deterioration. To prevent the deterioration of the pelvis, ideally fewer screws would be utilised to fixate the cup to the pelvis. However, in order to obtain fixation, currently fixation methods indicate that more screws are being utilised than required. This study presented results which provide evidence that certain screws are not required to obtain fixation which is proved by when the screws are suppressed, they do not alter the force distribution within the remaining screws. Within the perioperative plan, the results from this thesis can provide evidence that the screws with the least amount of force per millimetre of length do not have a significant impact on the force distribution within the remaining screws. This is supported by Chapter 5 which found that screws number 3 and 4 were not vital to obtain fixation intraoperatively and could be omitted from the perioperative plan to decrease further deterioration within the pelvis.

The screw plan (Appendix II) provides details on the length of each screw and if the screw is bicortical. A bicortical screw protrudes through to the other side of the pelvis where all bicortical screws have an estimated protrusion of 3mm. From the screw plan, only screws number 1 and 7 are not bicortical. Additionally, screw number 1 provides pubic fixation, screws number 2 and 3 provide ischial fixation and screws number 4, 5, 6 and 7 provide illial fixation. From a surgery point of view, with the screw plan suggested by OSSIS, intraoperatively the surgeon will need to get fixation of screw number 1 into the pelvis to gain pubic fixation, screw number 2 to gain ischial fixation and screws 5 – 7 to gain illial fixation. If any of these screws were not fixated adequately into the pelvis, there would be a significant increased risk of screw failure in one of the remaining screws as outlined in the results. Screws number 3 and 4 are the least crucial screws to get fixed into the pelvis and could be removed from the perioperative plan.

7.2 Limitations and Assumptions

Despite careful considerations when setting up the finite element model, there are limitations and assumptions that have been made in order to complete the study which are consistent with other finite element studies. Analysis has only been conducted under two different mechanical loading conditions, a nominal load and a peak contact force on the femoral head during a complete gait cycle. The transmission

of force into the screws under other applied loads within the hip during everyday activities may differ. The results have demonstrated that applying different loads to the femoral head can significantly alter the force distribution within the screws and the effect of suppressing one or two screws at a time under the different applied loads. The applied load in the second set of trial groups was adopted from Orthoload as a peak contact force on the femoral head during a complete gait cycle. The load applied was not subject-specific and did not consider the patient's weight and other varying factors that would alter the applied load on the femoral head during a complete gait cycle. The effect of other anatomical structures such as pelvic muscles, ligaments and tendons within the pelvis have not been modelled in order to simplify the model. The addition of these structures may alter the pelvic mechanics and effect the load transfer from the femoral head into the screws.

The study only represented the anatomy of one individual and the bone defects present for this case. The results produced are particular to the one patient and cannot be generalised for the entire population as they may not be reproducible for every person. Additionally, the number and orientation of the screws is only specific to the one subject. In the production process of a CTAC, the number and orientation of screws is selected and is subject specific depending on a number of factors. Therefore, the results produced in this study is only specific to the one patient and the force transmission into the screws may differ for other cases.

The material properties for both the bone graft and the pelvis was adopted from literature and not particular to the specific case. Assigning generalised material properties to both the bone graft and pelvis is a limitation as the properties assigned for each element may not represent the actual mechanical properties that exist within the bone. Due to time constraint and complexity, the material properties of the trabecular and cortical bone was not assessed from the grey scale on the CT scan. Homogeneous values of the material properties adopted from previous studies were used. It has been demonstrated in sensitivity studies of pelvic FEA models that utilising homogeneous properties produces similar results when compared to modelling with heterogeneous properties (Watson et al., 2018).

Since the pelvis that was studied in this thesis had significant bone defects, there would be a reduced amount of cortical bone in the actual pelvis compared to what was modelled. Shell elements of cortical bone was assigned in the model which would be over representation of the amount of cortical bone that is present in the pelvis. For this particular study, assigning shell elements of cortical bone is an assumption and an over generalisation of the amount of cortical bone that may be present in the actual pelvis. Assuming a constant thickness of the cortical bone has been adopted from previous studies (Anderson et al., 2005). The material properties assigned to the bone graft is also a limitation of the study since the actual material properties of the bone graft is variable depending on multiple factors. The amount of osseointegration of the bone graft into the pelvis has a significant effect on the material properties of this component. From

the graft material property verification study, the effect of the assigned Young's Modulus can alter the force distribution transmitted into the screws.

The results for the force distribution within the screws to determine primary fixation has not been validated experimentally. Experimentally testing the force distribution within the screws is challenging, particularly observing the effect of suppressing screws. A large amount of specimens would be required to achieve the results that was produced in this study. An effort was made to ensure that the geometry, material properties and the setup of the finite element model including applied load and boundary conditions realistically represented the mechanical environment within the pelvis. However, there are always limitations associated with these aspects, with particular mention of the mesh assignment. Although a mesh refinement study was performed, there are limitations associated with the mesh accurately representing the geometry.

7.3 Future Work

The results presented in this study provides an initial insight into the mechanical environment within the screws under two applied loads. Understanding the transmission of applied load into the screws and the effect of suppressing screws can provide surgeons with the knowledge of which screws are more important to gain fixation intraoperatively to reduce the risk of both screw and implant failure. With the foundations of this study, there is scope for future development to reduce the limitations associated and to further gain an enhanced understanding of the mechanical environment within the screws.

The material properties of the pelvis can be obtained using the CT scan of the subject. Utilising the greyscale values on a CT scan can determine the mechanical properties of the pelvis as discussed in Chapter 2. The Young's Modulus can be calculated using the apparent density of the bone tissue which would increase the validity of the results using subject specific material properties. Assigning the material properties of the pelvis to be subject specific would reduce the limitation of utilising a constant thickness of cortical bone and would accurately represent the bone deficiencies on a greater scale.

To represent a larger cohort of cases that present with bone deficiencies requiring a CTAC, generating results utilising different bone geometry and implant designs can create a wider understanding on the mechanical environment within the screws. Altering the screw plan to incorporate varying screw lengths and orientation could aid in the reduction of the number of screws utilised to fixate the implant to the host bone. Performing finite element analysis on a range of CTAC designs with varying screw plans may be able to produce an optimal number of screws that would be utilised to gain fixation of the implant to bone. In addition to this, a generalisation could be made in association with the number of screws required in the three flanges depending on the type and severity of bone defects in the pelvis.

Improvements could be made to the finite element model, in particular the applied load. Applying a load to the surface of the femoral head that is patient specific could provide more accurate results on the force transmitted into the screws. Since the forces in the hip joint can vary significantly depending on the type of activity and subject specific variables such as hip biomechanics, age, fitness and weight, it is difficult to be able to perform analyses for all types of activities. Preferably, hip joint forces would be collected prior to surgery in the healthy hip while performing everyday activities for a certain period of time to determine the loads that would be transmitted onto the femoral head. Having data that is subject specific would provide information on the joint forces which may simulate the loads the screws would encounter post operatively.

8 Conclusion

This study presented an analytical method to determine the force distribution within the screws that are utilised to fixate a custom tri-flange acetabular component to the pelvis. The transmission of force from the applied load under two mechanical conditions was sought. The results provided evidence to suggest that out of the 7 screws, suppressing screws number 3 and 4 under the peak contact force during a complete gait cycle had the least effect on the force distribution within the remaining screws. The screw plan could be altered to remove screws number 3 and 4 within the perioperative plan which would ultimately aid in the restoration of the poor bone quality found within the pelvis. Removing one or two screws from the screw plan reduces the number of screw holes required within the already fragile bone, hence improving the bone quality and help aid the both the patient's recovery and bone health.

9 References

- Absel, M, Trousdale, R, Berry, 'Pelvic Discontinuity Associated With Total Hip Arthroplasty: Evaluation and Management'. *Journal of the American Academy of Orthopaedic Surgeons*. Vol. 25, pp. 330-338.
- Anderson, A, Peters, C, Tuttle, B, Weiss, J (2005). 'A Subject-Specific Finite Element Model of the Pelvis: Development, Validation and Sensitivity Studies'. *Journal of Biomechanical Engineering*. Vol. 127, no. 3, pp. 364-373.
- Armentia, M, Abasolo, M, Coria, I, Albizuri, J (2020). 'Fatigue Design of Dental Implant Assemblies: A Nominal Stress Approach'. *Metals*. Vol. 10, no. 744.
- Baaui, M, Hellemond, G, Hooff, M, Spruit, M (2015). 'The accuracy of positioning a custom-made implant within a large acetabular defect at revision arthroplasty of the hip'. *The Bone and Joint Journal*. Vol. 97, pp. 780-785.
- Barlow, B, Oi, K, Lee, Y, Carli, A, Choi, D, Bostrom, M (2016). 'Outcomes of Custom Flange Acetabular Components in Revision Total Hip Arthroplasty and Predictors of Failure'. *The Journal of Arthroplasty*. Vol. 31, pp. 1057-1064.
- Batista, V, Verri, F, Almeida, F, Santiago, J, Lemos, C, Pellizzer, E (2017). 'Finite element analysis of implant-supported prosthesis with pontic and cantilever in the posterior maxilla'. *Computer methods in Biomechanics and Biomedical Engineering*. Vol. 20, no. 6, pp. 663-670.
- Berasi, C, Berend, K, Adams, J, Ruh, E, Lombardi, A (2014). 'Are custom triflange acetabular components effective for reconstruction of catastrophic bone loss?'. *Clinical Orthopaedics and Related Research*. Vol. 473, pp. 528-535.
- Berend, M, Berend, K, Lombardi, A, Cates, H, Faris, P (2018). 'The patient-specific Triflange acetabular implant for revision total hip arthroplasty in patients with severe acetabular defects'. *The Bone & Joint Journal*. No. 100-B, pp. 50-54.
- Chatzistergos, P, Magnissalis, E, Kourkoulis, S (2010). 'A parametric study of cylindrical pedicle screw design implications on the pullout performance using an experimentally validated finite element model'. *Staffordshire Online Repository*. Available at: https://core.ac.uk/reader/18269289?utm_source=linkout (Accessed 18th May 2022).
- Christie, M (2016). 'Triflange Cup'. *Musculoskeletal Key*. Available at: <https://musculoskeletalkey.com/triflange-cup/> (Accessed: 18th May 2022).

- Damm, P, Bender, A, Bergmann, G (2015). 'Postoperative Changes in In Vivo Measured Friction in Total Hip Joint Prosthesis during Walking'. *PLOS One*. Vol. 10, no. 1371.
- Didier, P, Piotrowski, B, Coz, G, Joseph, D, Bravetti, P, Laheurte, P (2020). 'Finite element analysis of the stress field in peri-implant bone: a parametric study of influencing parameters and their interactions for multi-objective optimisation'. *Applied Sciences*. Vol. 10, no. 5973.
- Dong, E, Wang, L, Iqbal, T, Dichen, L, Liu, Y, He, J, Zhao, B, Li, Y (2018). 'Finite Element Analysis of the Pelvis after Customized Prosthesis Reconstruction'. *Journal of Bionic Engineering*. Vol. 15, pp. 443-451.
- Eemeren, A, Vanlommel, J, Vandekerckhove, M (2020). 'Acetabular reconstruction with a custom-made triflange acetabular component through direct anterior approach – A case report'. *Journal of clinical orthopedics and trauma*. Vol. 11, pp. 211-213.
- Finnila, S, Moritz, N, Svedstrom, E, Alm, J, Aro, H (2015). 'Increased micromotion of uncemented acetabular cups in female total hip arthroplasty patients with low systemic bone mineral density'. *Acta Orthopaedica*. Vol. 87, pp. 48-54.
- Froschen, F, Randau, T, Hischebeth, G, Gravius, N, Wirtz, D, Gravius, S, Walter, S (2020). 'Outcome of repeated multi-stage arthroplasty with custom-made acetabular implants in patients with severe acetabular bone loss: a case series'. *HIP International*. Vol. 30, pp. 64-71.
- Gladnick, B, Fehring, K, Odum, S, Christie, M, DeBoer, D, Fehring, T (2018). 'Midterm Survivorship After Revision Total Hip Arthroplasty With a Custom Triflange Acetabular Component'. *The Journal of Arthroplasty*. Vol. 33, pp. 500-504.
- Goodman, G (2016), 'The custom triflange cup'. *The Bone and Joint Journal*. Vol. 98, pp. 68-72.
- Gruber, M, Jasenko, M, Burghuber, J, Hochreiter, J, Ritschl, P, Ortmaier, R (2020). 'Functional and radiological outcomes after treatment with custom-made acetabular components in patients with Paprosky type 3 acetabular defects: short term results'. *BMC Musculoskeletal Disorders*. Vol. 20, no. 835.
- Helgason, B, Perilli, E, Schileo, E, Taddei, F, Brynjolfsson, S, Viceconti, M (2007). 'Mathematical relationships between bone density and mechanical properties: A literature review'. *Clinical Biomechanics*. Vol. 23, pp. 135-146.
- Holt, G, Dennis, D (2004). 'Use of custom triflanged acetabular components in revision total hip arthroplasty'. *Clinical orthopaedics and related research*. No. 429, pp. 209-214.

- Iqbal, T, Shi, L, Wang, L, Liu, Y, Li, D, Qin, M, Jin, Z (2017). 'Development of finite element model for customized prostheses design for patient with pelvic bone tumour', *Journal of Engineering in Medicine*, vol. 23, no. 6, pp. 525-533.
- Isaac, G, Brockett, C, Breckon, A, Jagt, D, Williams, S, Hardaker, C, Fisher, J, Schepers, A (2009). 'Ceramic-on-metal bearings in total hip replacement'. *The Journal of Bone and Joint Surgery*. Vol. 91, pp. 1134-1141.
- Kaku, N, Tanaka, A, Tagomori, H, Tsumura, H (2019). 'Finite Element Analysis of Stress Distribution in Flat and Elevated-Rim Polyethylene Acetabular Liners'. *Clinics in Orthopedic Surgery*. Bol. 12, pp. 291-297.
- Kosashvili, Y, Backstein, D, Safir, O, Lakstien, D, Gross A (2009). 'Acetabular revision using an anti-protrusion (ilio-ischial) cage and trabecular metal acetabular component for severe acetabular bone loss associated with pelvic discontinuity'. *The Journal of Bone and Joint Surgery*. Vol. 91, pp. 870-876.
- Kotela, A, Lorkowski, J, Chmielewski, D, Grodzik, M, Kotela, I (2020). 'Revision Hip Arthroplasty in Patient with Acetabulum Migration into Subperitoneal Space – A Case Report'. *Medicina*. Vol. 57, no. 30.
- Maslov, L, Borovkov, A, Maslova, I, Soloviev, D, Zhmaylo, M, Tarasenko, F (2021). 'Finite Element Analysis of Customized Acetabular Implant and Bone after Pelvic Tumour Resection throughout the Gait Cycle'. *Materials*. Vol. 14, no. 7066.
- Maslov, L, Surkova, P, Maslova, I, Solovev, D, Zhmaylo, M, Kovalenko, A, Bilyk, S (2019). 'Finite-element study of the customized implant for revision hip replacement'. *JVE Journals*. Available at: <https://www.extrica.com/article/20961> (Accessed: 6 April 2022)
- Matar, H, Selvaratnam, V, Shah, N, Jones, H (2020). 'Custom triflange revision acetabular components for significant bone defects and pelvic discontinuity: Early UK experience', *Journal of Orthopaedics*, vol. 21, pp. 25-30.
- Mathes, S (2015). 'Removal of Implanted Metal – Hardware removal: A Guide to Recovery after Surgery'. *Rebalance*. Available at: https://rebalancemd.com/wp-content/uploads/2017/08/Hardware_removal_Recovery_Guide.pdf (Accessed: 18th May 2022).
- Martino, I, Strigelli, V, Cacciola, G, Gu, A, Bostrom, M, Sculco, P (2019). 'Survivorship and Clinical Outcomes of Custom Triflange Acetabular Components in Revision Total Hip Arthroplasty: A Systematic Review', *The Journal of Arthroplasty*, vol. 34, pp. 2511-2518.

- Moazan, M, Mak, J, Jones, A, Jin, Z, Wilcox, R, Tsiridis, E (2013). 'Evaluation of a new approach for modelling the screw–bone interface in a locking plate fixation: A corroboration study'. *Journal of Engineering in Medicine*. Vol. 227, no. 7, pp. 746-756.
- Myncke, I, Schaik, D, Scheerlinck (2017). 'Custom-made triflanged acetabular components in the treatment of major acetabular defects. Short-term results and clinical experience', *Acta Orthopaedica Belgica*, vol. 83, no. 3, pp. 341-350.
- Nieminen, J, Pakarinen, T, Laitinen, M (2013). 'Orthopaedic reconstruction of complex pelvic bone defects. Evaluation of various treatment methods'. *Scandinavian Journal of Surgery*. Vol/ 102, pp. 36-41.
- Palmowski, Y, Popovic, S, Schuster, S, Hardt, S, Damm, P (2021). 'In vivo analysis of hip joint loading on Nordic walking novices'. *Journal of Orthopaedic Surgery and Research*. Vol. 16, no. 596.
- Razi, T, Manaf, N, Yadekar, M, Razi, S, Gheibi, S (2019). 'Correction of Cupping Artifacts in Axial Cone-Beam Computed Tomography Images by Using Image Processing Algorithms'. *Journal of Advanced Oral Research*. Vol. 10, no. 2, pp. 132-136.
- Rho, Y, Hobatho, M, Ashman, R (2005). 'Relations of mechanical properties to density and CT numbers in human bone'. *Medical Engineering and Physics*. Vol. 17, no. 5, pp. 347-355.
- Roberts, T, Rosenbaum, A (2012). 'Bone grafts, bone substitutes and orthobiologics, the bridge between basic science and clinical advancements in fracture healing'. *Organogenesis*. Vol. 8, no. 4, pp. 114-124.
- Samanthi, D (2013). 'Difference between Pelvis and Pelvic Girdle', *Difference Between*. Available at: <https://www.differencebetween.com/difference-between-pelvis-and-vs-pelvic-girdle/> (Accessed: 18th May 2022).
- Sershon, R, McDonald, J, Nagda, S, Hamilton, W, Engh, C (2021). 'Custom triflange cups: 20-year experience'. *The Journal of Arthroplasty*. Vol. 36, pp. 3264-3268.
- Steiner, J, Ferguson, S, Lenthe, H (2014). 'Computational analysis of primary implant stability in trabecular bone'. *Journal of Biomechanics*. Vol. 48, pp. 807-815.
- Sulco, P, Wright, T, Malahias, M, Gu, A, Bostrom, M, Haddad, F, Jerabek, S, Bolognesi, M, Fehring, T, DellaValle, A, Jiranek, W, Walter, W, Paprosky, W, Garbuz, D, Sculco, T (2022). 'The Diagnosis and Treatment of Acetabular Bone Loss in Revision Hip Arthroplasty: An International Consensus Symposium', *The Musculoskeletal Journal of Hospital for Special Surgery*, vol. 18, no. 1, pp. 8-41.

- Taunton, M, Fehring, T, Edwards, P, Bernasek, T, Holt, G, Christie, M (2012). 'Pelvic discontinuity treated with custom triflange component'. *Clinical Orthopaedics and Related Research*. Vol. 470, pp. 428-434.
- Totoribe, K, Chosa, E, Yamako, G, Hamada, H, Ouchi, K, Yamashita, S, Deng, G (2018). 'Finite element analysis of the tibial bone graft in cementless total knee arthroplasty'. *Journal of Orthopaedic Surgery and Research*. Vol. 13, no. 113.
- Waddell, B, Boettner, F, Valle, A (2017). 'Favorable early results of impaction bone grafting with reinforcement mesh for the treatment of paprosky 3D acetabular defects'. *The Journal of Arthroplasty*. Vol. 32, pp. 919-923.
- Watson, P, Dostanpor, A, Fagan, M, Dobson, C (2018). 'The effect on boundary constraints on finite element modelling of the human pelvis'. *Elsevier*. Available at: <file:///userref/f/fair0135/Downloads/2018-03-01%2014733%20Watson.pdf> (Accessed: 18th May 2022).
- Wieding, J, Souffrant, R, Fritsche, A, Mittelmeier, W, Bader, R (2012). 'Finite Element Analysis of Osteosynthesis Screw Fixation in the Bone Stock: An Appropriate Method for Automatic Screw Modelling', *PLoS One*, vol. 7, no. 3.
- Wind, M, Swank, M, Sorger, J (2013). 'Short term results of a custom triflange acetabular component for massive acetabular boss loss in revision THA'. *Healio*. Vol. 36, no. 3.
- Zanasa, S, Zmerly, H (2020). 'Customised three-dimensional printed revision acetabular implant for large defect after failed triflange revision cup'. *BMJ Innovations in treatment*. Vol. 13, no. 233965.
- Voor, M, Nawab, A, Malkani, A, Ullrich, C (2000). 'Mechanical properties of compacted morselized cancellous bone graft using one-dimensional consolidation testing'. *Journal of Biomechanics*. Vol. 33, pp. 1683-1688.
- Zimmer Biomet (2011). 'Titanium Locking Screw for Triflange Acetabular component'. Available at: <https://www.zimmerbiomet.com/content/dam/zb-corporate/en/products/specialties/hip/triflange/titanium-locking-screw-for-triflange-acetabular-component-surgical-technique.pdf> (Accessed: 18th May 2022).
- Zimmer Biomet (2022). 'Triflange Acetabular component'. Available at: <https://www.zimmerbiomet.com/en/products-and-solutions/specialties/hip/triflange-acetabular-component.html> (Accessed: 18th May 2022).

10 Appendices

Appendix I: Illustration of the human pelvic girdle

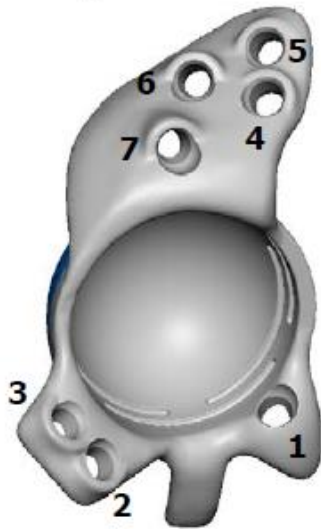
Figure removed due to copyright restriction

Figure 10.1: Pelvic Girdle (Samanthi, 2013)

Appendix II: Screw Plan

Screw Lengths

Screw length measurement has been calculated as follows:



Screw	Length(mm)*	Bicortical	Estimated Protrusion
1	31	NO	0mm
2	25	YES	3mm
3	32	YES	3mm
4	28	YES	3mm
5	22	YES	3mm
6	31	YES	3mm
7	59	NO	0mm

Figure 10.2: Screw Plan with Lengths

Appendix III: Mesh Generation

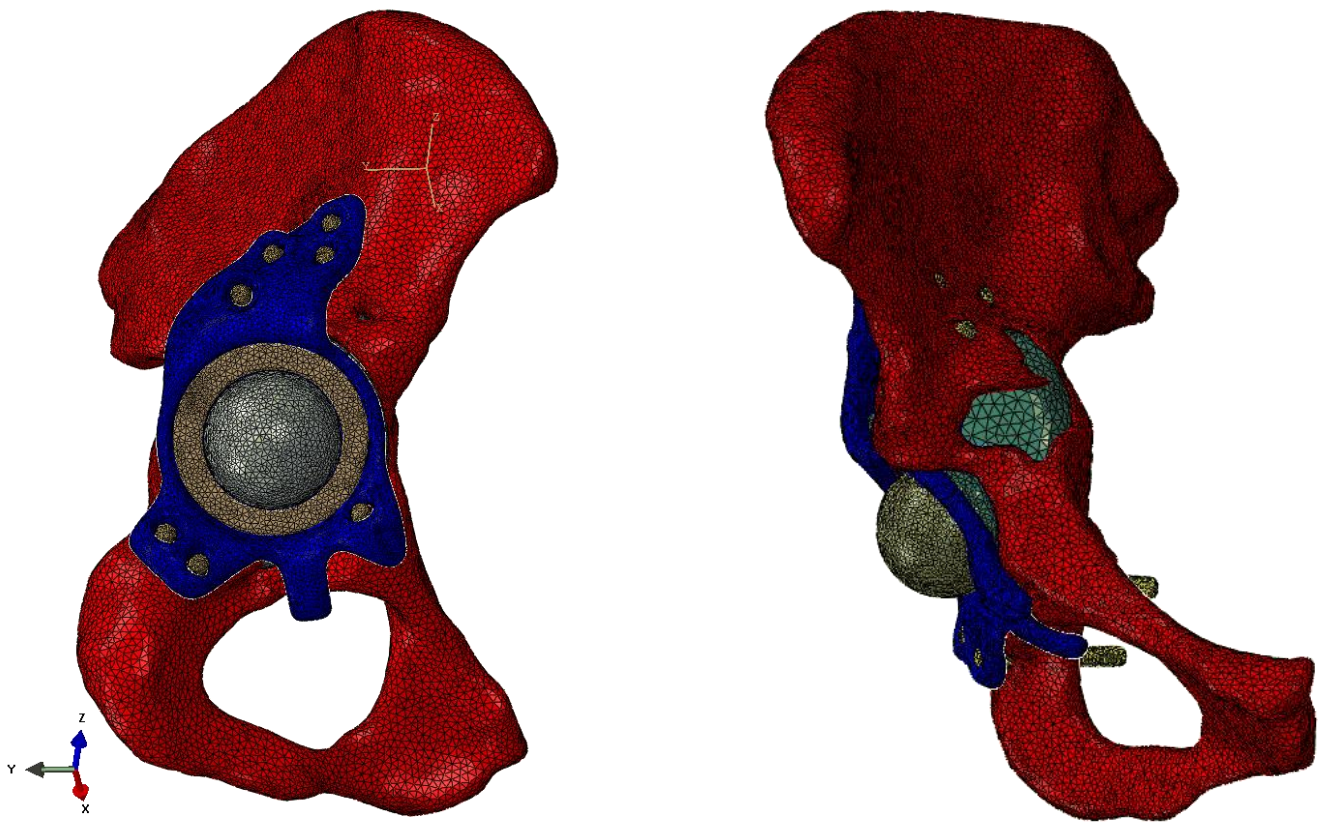


Figure 10.3: Mesh generation on all components

Appendix IV: Mesh Properties

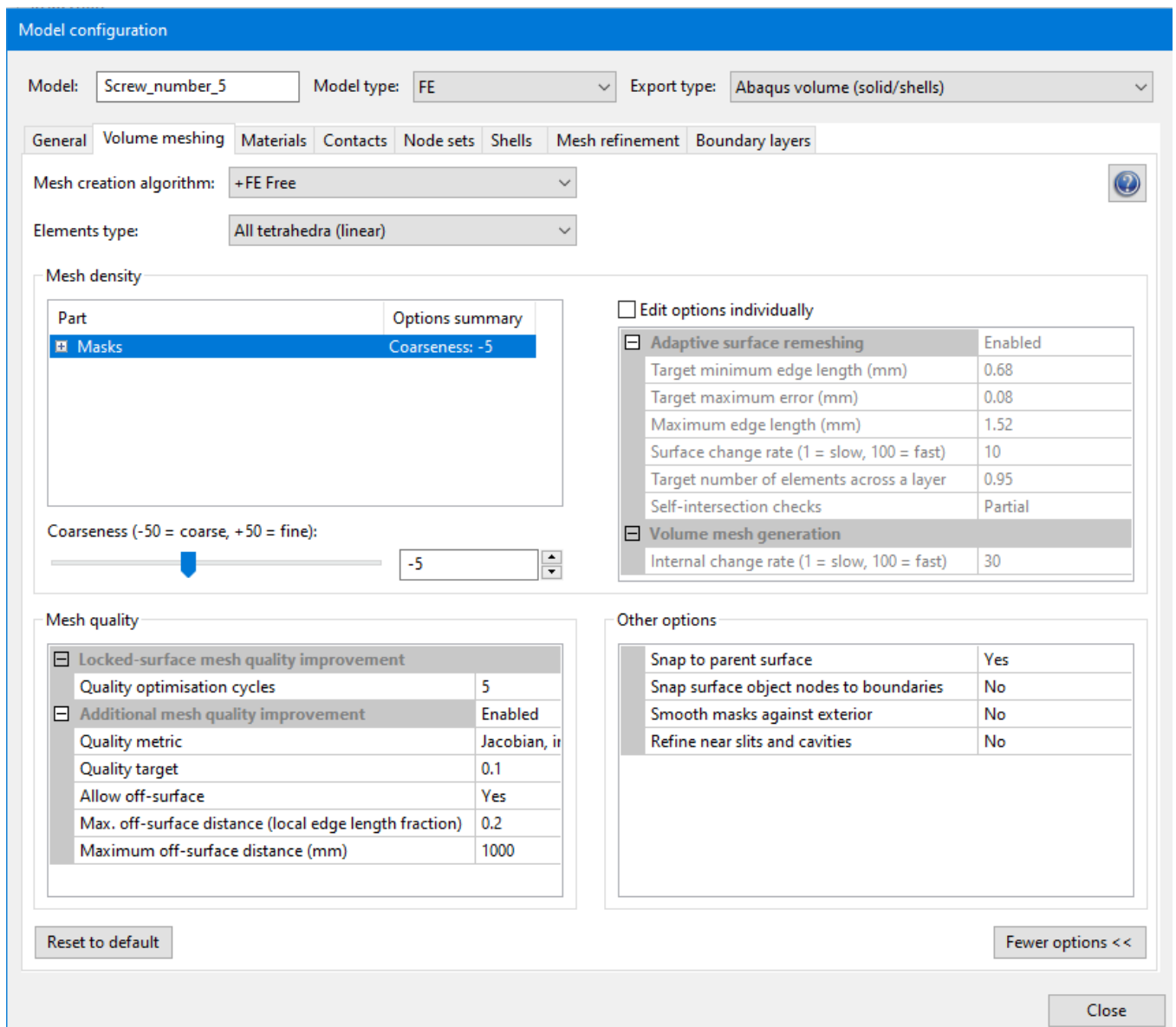


Figure 10.4: Mesh properties for coarseness set to -5

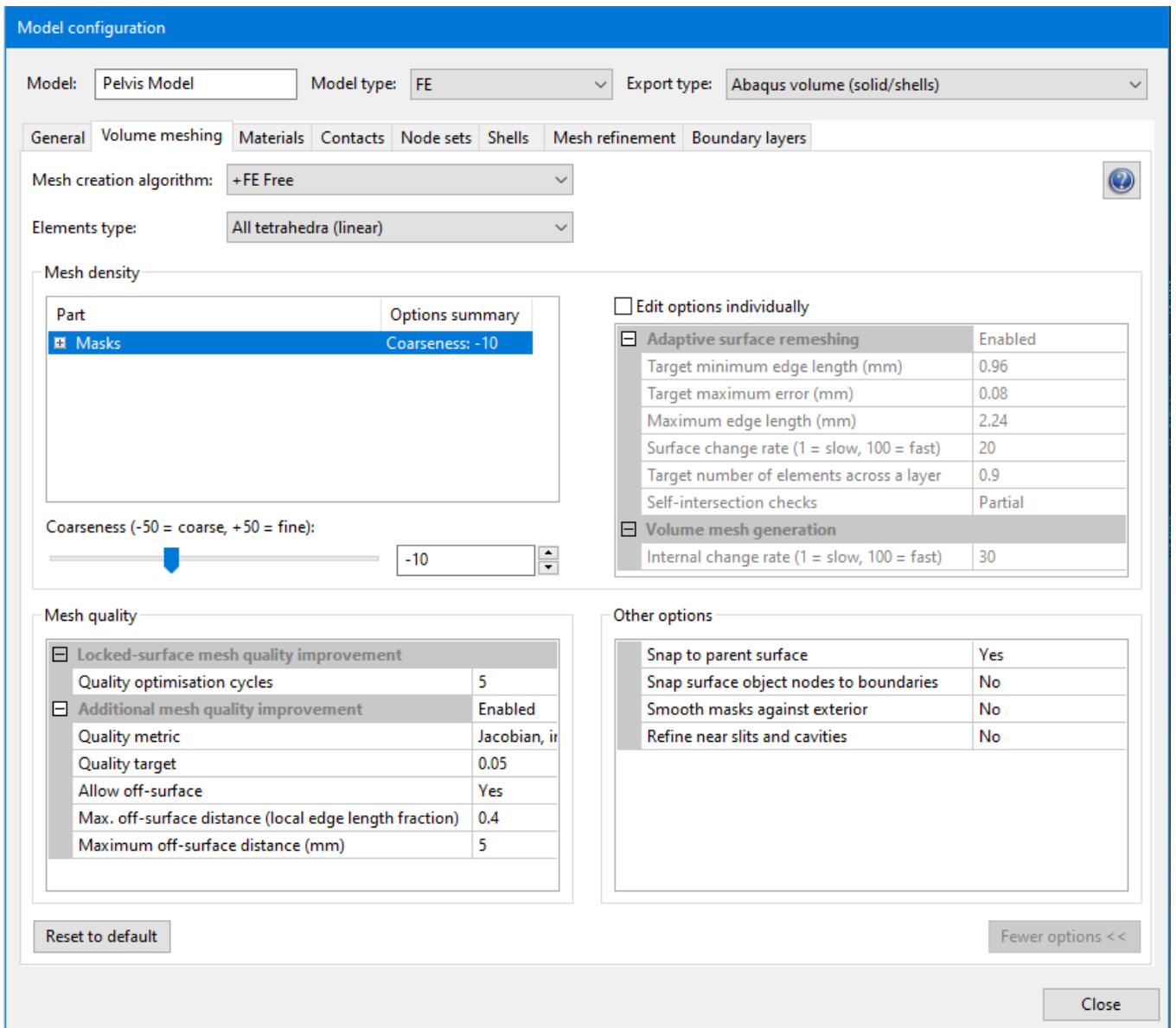


Figure 10.5: Mesh properties for coarseness set to -10

Model configuration

Model: Model type: Export type:

General Volume meshing Materials Contacts Node sets Shells Mesh refinement Boundary layers

Mesh creation algorithm:

Elements type:

Mesh density

Part	Options summary
Masks	Edited individually

Coarseness (-50 = coarse, +50 = fine):

Edit options individually

<input type="checkbox"/> Adaptive surface remeshing	Enabled
Target minimum edge length (mm)	0.368
Target maximum error (mm)	0.072
Maximum edge length (mm)	1.386667
Surface change rate (1 = slow, 100 = fast)	56
Target number of elements across a layer	1.8
Self-intersection checks	None
<input type="checkbox"/> Volume mesh generation	
Internal change rate (1 = slow, 100 = fast)	24

Mesh quality

<input type="checkbox"/> Locked-surface mesh quality improvement	
Quality optimisation cycles	5
<input type="checkbox"/> Additional mesh quality improvement	Enabled
Quality metric	Jacobian, i
Quality target	0.1
Allow off-surface	Yes
Max. off-surface distance (local edge length fraction)	0.2
Maximum off-surface distance (mm)	1000

Other options

Snap to parent surface	Yes
Snap surface object nodes to boundaries	No
Smooth masks against exterior	No
Refine near slits and cavities	No

Figure 10.6: Mesh properties for coarseness set to +10

Appendix V: MATLAB Code

```

%% Extracting force in each part into table

data=readcell('31032022_29.xlsx');
trial=29;

trialno=num2cell(trial);

data2=data;

%% Getting Part Names

partid=find(strcmp(data2(:,3),'reported'));

noparts=size(partid);
noparts=noparts(1);

for i=1:noparts

    row=partid(i);
    results2(i,1)=data2(row,9);

end

%% Getting total force in each part

endpart=find(strcmp(data2(:,2),'Total'));

for i=2:(noparts+1)

    if results2(i-1)=="SCREW1-1#PART-1-1"

        row=endpart(i-1);
        results(2,(2))=data2(row,4);
        results(2,(3))=data2(row,5);
        results(2,(4))=data2(row,6);
        x=cell2mat(results(2,2));
        x1=isempty(x);
        y=cell2mat(results(2,3));
        y1=isempty(y);
        z=cell2mat(results(2,4));
        z1=isempty(z);

        if x1==1
            x=0;
        elseif y1==1
            y=0;
        elseif z1==1
            z=0;
        end

        results(2,(5))=num2cell(sqrt(x^2+y^2+z^2));
        result_final(2,(trial+1))=num2cell(sqrt(x^2+y^2+z^2));

    end

    if results2(i-1)=="SCREW2-1#PART-1-1"

```

```

row=endpart(i-1);
results(3,(2))=data2(row,4);
results(3,(3))=data2(row,5);
results(3,(4))=data2(row,6);
x=cell2mat(results(3,2));
x1=isempty(x);
y=cell2mat(results(3,3));
y1=isempty(y);
z=cell2mat(results(3,4));
z1=isempty(z);

if x1==1
    x=0;
elseif y1==1
    y=0;
elseif z1==1
    z=0;
end
results(3,(5))=num2cell(sqrt(x^2+y^2+z^2));
result_final(3,(trial+1))=num2cell(sqrt(x^2+y^2+z^2));
end

if results2(i-1)=="SCREW3-1#PART-1-1"

row=endpart(i-1);
results(4,(2))=data2(row,4);
results(4,(3))=data2(row,5);
results(4,(4))=data2(row,6);
x=cell2mat(results(4,2));
x1=isempty(x);
y=cell2mat(results(4,3));
y1=isempty(y);
z=cell2mat(results(4,4));
z1=isempty(z);

if x1==1
    x=0;
elseif y1==1
    y=0;
elseif z1==1
    z=0;
end

results(4,(5))=num2cell(sqrt(x^2+y^2+z^2));
result_final(4,(trial+1))=num2cell(sqrt(x^2+y^2+z^2));
end

if results2(i-1)=="SCREW4-1#PART-1-1"

row=endpart(i-1);
results(5,(2))=data2(row,4);
results(5,(3))=data2(row,5);
results(5,(4))=data2(row,6);
x=cell2mat(results(5,2));
x1=isempty(x);
y=cell2mat(results(5,3));
y1=isempty(y);
z=cell2mat(results(5,4));
z1=isempty(z);

```



```

if x1==1
    x=0;
elseif y1==1
    y=0;
elseif z1==1
    z=0;
end
results(5, (5))=num2cell(sqrt(x^2+y^2+z^2));
result_final(5, (trial+1))=num2cell(sqrt(x^2+y^2+z^2));
end

if results2(i-1)=="SCREW5-1#PART-1-1"

    row=endpart(i-1);
    results(6, (2))=data2(row, 4);
    results(6, (3))=data2(row, 5);
    results(6, (4))=data2(row, 6);
    x=cell2mat(results(6, 2));
    x1=isempty(x);
    y=cell2mat(results(6, 3));
    y1=isempty(y);
    z=cell2mat(results(6, 4));
    z1=isempty(z);

    if x1==1
        x=0;
    elseif y1==1
        y=0;
    elseif z1==1
        z=0;
    end
    results(6, (5))=num2cell(sqrt(x^2+y^2+z^2));
    result_final(6, (trial+1))=num2cell(sqrt(x^2+y^2+z^2));
end

if results2(i-1)=="SCREW6-1#PART-1-1"

    row=endpart(i-1);
    results(7, (2))=data2(row, 4);
    results(7, (3))=data2(row, 5);
    results(7, (4))=data2(row, 6);
    x=cell2mat(results(7, 2));
    x1=isempty(x);
    y=cell2mat(results(7, 3));
    y1=isempty(y);
    z=cell2mat(results(7, 4));
    z1=isempty(z);

    if x1==1
        x=0;
    elseif y1==1
        y=0;
    elseif z1==1
        z=0;
    end
    results(7, (5))=num2cell(sqrt(x^2+y^2+z^2));
    result_final(7, (trial+1))=num2cell(sqrt(x^2+y^2+z^2));
end

if results2(i-1)=="SCREW7_1-1#PART-1-1"

    row=endpart(i-1);

```

```
results(8,(2))=data2(row,4);
results(8,(3))=data2(row,5);
results(8,(4))=data2(row,6);
x=cell2mat(results(8,2));
x1=isempty(x);
y=cell2mat(results(8,3));
y1=isempty(y);
z=cell2mat(results(8,4));
z1=isempty(z);

if x1==1
    x=0;
elseif y1==1
    y=0;
elseif z1==1
    z=0;
end
results(8,(5))=num2cell(sqrt(x^2+y^2+z^2));
result_final(8,(trial+1))=num2cell(sqrt(x^2+y^2+z^2));
end
end
```

Appendix VI: Gantt Chart

A Gantt Chart is produced showing the project deliverables and associated dates. It is important to have a flexible Gantt Chart but stick to the key dates to be able to adapt to changes in the timeline when issues arise throughout the project.

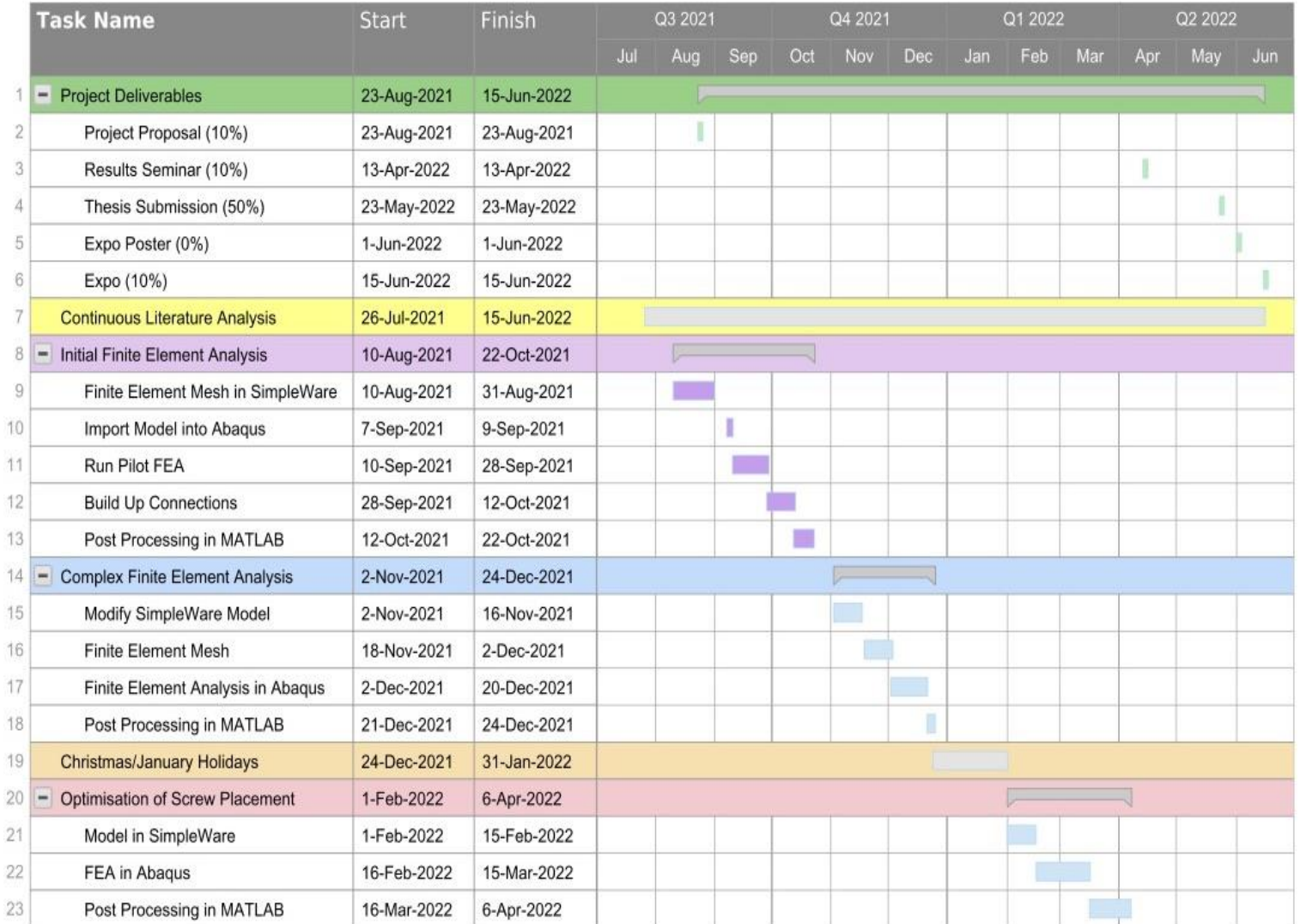


Figure 10.7: Gantt Chart